ELSEVIER

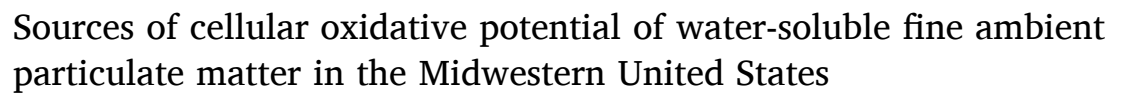
Contents lists available at ScienceDirect

Journal of Hazardous Materials

journal homepage: www.elsevier.com/locate/jhazmat



Research Paper



Yixiang Wang, Joseph V. Puthussery, Haoran Yu, Yicen Liu, Sudheer Salana, Vishal Verma

Department of Civil and Environmental Engineering, University of Illinois at Urbana-Champaign, 205 North Mathews Avenue, Urbana, IL 61801, United States



ARTICLE INFO

Editor: Dr. H. Zaher

Keywords:
Cellular oxidative potential
Midwestern United States
Source apportionment
Positive matrix factorization
Spatiotemporal distribution

ABSTRACT

We investigated the spatiotemporal distribution and sources of cellular oxidative potential (OP) in the Midwest US. Weekly samples were collected from three urban [Chicago (IL), Indianapolis (IN), and St. Louis (MO)], one rural [Bondville (IL], and one roadside site [Champaign (IL)] for a year (May 2018 to May 2019), and analyzed for water-soluble cellular OP using a macrophage reactive oxygen species (ROS) assay. Chemical composition of the samples including several carbonaceous components, inorganic ions, and water-soluble elementals, were also analyzed. The emission sources contributing to water-soluble cellular OP and $PM_{2.5}$ mass were analyzed using positive matrix factorization. The secondary organic aerosols contributed substantially (\geq 54%) to $PM_{2.5}$ cellular OP a turban sites, while the roadside and rural OP were dominated by road dust (54%) and agricultural activities (62%), respectively. However, none of these sources contributed substantially to the $PM_{2.5}$ mass (\leq 21%). Other sources contributing significantly to the $PM_{2.5}$ mass, i.e., secondary sulfate and nitrate, biomass burning and coal combustion (14–26%) contributed minimally to the cellular OP (\leq 13%). Such divergent profiles of the emission sources contributing to cellular OP vs. $PM_{2.5}$ mass demonstrate the need of considering more health-relevant metrics such as OP in the design of air pollution control strategies.

1. Introduction

Ambient particulate matter (PM) has been related to pulmonary disorders (Holst et al., 2020; Pun et al., 2017), cardiovascular disease (Cesaroni et al., 2014; Tian et al., 2019), kidney cancer (Raaschou-Nielsen et al., 2017; Turner et al., 2017), stroke (Huang et al., 2019; Shah et al., 2015), and even dementia (Chen et al., 2017; Underwood, 2017). The particles with a diameter less than 2.5 µm are especially hazardous because they can penetrate the respiratory system and deposit inside the lungs (Miller et al., 1979). Owing to the strong relationships between PM_{2.5} and various health effects, and given the ease of measurement, mass concentrations have been used as the national ambient air quality standards (NAAQS) to regulate ambient PM2.5. However, even after NAAQS implementation for more than three decades, more than 50 million people in the US currently live in the areas with PM_{2.5} exceeding the standards (12 μ g/m³) of annual mean PM_{2.5} concentrations (EPA, 2021). Many of these regions are in the midwestern United States, such as Chicago, IL and Indianapolis, IN (Hu et al., 2017). Not surprisingly, the Midwestern urban area has one of the highest percentage (5-7%) of premature mortality related to PM_{2.5} in the US (Fann et al., 2018). A better identification of $PM_{2.5}$ sources and assessing their health risks in the Midwest US can probably help to reduce these mortalities.

As sources of PM_{2.5} could vary a lot among different locations, implementing an efficient PM2.5 control plan requires a good understanding of the regional emission sources. Source apportionment models such as positive matrix factorization (PMF) and chemical mass balance (CMB), have been applied to track the PM_{2.5} sources in the Midwest US. For example, Milando et al. (2016) used PMF to investigate 15 years (2001-2015) trend of PM2.5 contributors in Detroit and Chicago, and found secondary sulfate, secondary nitrate, vehicular emissions and biomass burning as the major sources contributing to PM2.5 mass. In addition to these sources, industrial emissions also exerted a significant impact on the PM_{2.5} in certain urban areas of the Midwest. Industrial metal-rich sources such as metals (zinc, copper and lead) smelting and steel processing were found to contribute 7-15% to the PM_{2.5} mass concentration in urban areas of St. Louis, MO in 2000-2003 (Amato and Hopke, 2012). In contrast, there are very few primary sources of PM_{2.5} in the rural areas. Kim et al. (2005) showed an overwhelming role of secondary sulfate and nitrate, contributing to more than 80% of the $\mbox{PM}_{2.5}$

E-mail address: vverma@illinois.edu (V. Verma).

^{*} Corresponding author.

mass concentration at a rural site (Bondville, IL) in the Midwest US.

It is important to note that all the sources contributing to the PM_{2.5} mass do not necessarily contribute to the health effects. For example, Krall et al. (2017) selected four U.S. cities (Atlanta, GA, Birmingham, AL, St. Louis, MO, and Dallas, TX) to link anthropogenic emission sources with emergency department (ED) visits for respiratory diseases (e.g., pneumonia, chronic obstructive pulmonary disease, upper respiratory infection, and asthma.). For St. Louis metropolitan area, biomass burning, diesel vehicle, and dust contributed significantly to the PM_{2.5} mass concentration, however, only biomass burning was positively associated with respiratory effects [relative risk (RR)= 1.007; 95% confidence intervals (CI): 0.999, 1.016]. These differences are probably because not all components of the ambient PM2.5 are equally toxic. This is further demonstrated in another epidemiological study conducted in St. Louis to investigate PM_{2.5} components' associations with cardiovascular diseases-related ED visits (Sarnat et al., 2015). The association of ED visits with organic carbon (OC) was found to be stronger [RR= 1.036 (95% CI: 1.001, 1.072)] than the PM_{2.5} mass concentration [RR= 1.015 (95% CI: 0.980, 1.051)]. These studies are consistent with the findings from our lab showing significant correlations of cytotoxicity of ambient PM25 collected from a midwestern site with only a few components of the PM_{2.5}, particularly water-soluble organic carbon (WSOC), Fe, and Cu (Wang, Y. et al., 2018). Therefore, to better protect the public health from the harmful effects of ambient PM2.5, we have to shift our perspective from bulk mass to intrinsically toxic PM2.5 components.

Given that PM_{2.5} toxicity is a not very well understood phenomenon, some guidance can be obtained from the initiating steps in PM_{2.5} toxicity ladder, which is the generation of reactive oxygen species (ROS) (Deng et al., 2013; Feng et al., 2016). Both cellular and acellular assays exist to measure the capability of ambient PM to generate ROS. The examples of chemical assays are dithiothreitol (DTT) assay (Kumagai et al., 2002; Li et al., 2003a, 2003b), ascorbate assay (Mudway et al., 2005, 2004), glutathione (GSH) assay (Zielinski et al., 1999), and hydroxyl radicals (OH) generation in a surrogate lung fluid (SLF) (Charrier et al., 2014; Vidrio et al., 2009), while researchers have most commonly used alveolar macrophages to assess the cellular generation of ROS (Delfino et al., 2013; Hamad et al., 2016; Hiura et al., 1999; Landreman et al., 2008; Wang et al., 2013; Zhang et al., 2008). Despite more strenuous protocols of the cellular assays, cellular generation of ROS probably offers a more accurate representation of the capability of PM2.5 in inducing the health effects than the chemical assays. The overall capability of ambient PM_{2.5} to either oxidize the antioxidants/reductants or catalyze the production of ROS is conveniently called the oxidative potential (OP) or ROS

Compared to the mass concentration, PM2.5 OP could be a more relevant metric to represent PM toxicity. Therefore, there is an emerging trend of involving OP in PM_{2.5} source apportionment studies. These studies have come from different geographical regions of the world such as Beijing (DTT assay) (Ma et al., 2018; Yu et al., 2019), Xi'an (DTT assay) (Wang et al., 2020), Wuhan (DTT assay) (L. Liu et al., 2020; Q.Y. Liu et al,. 2020), coastal cities (Jinzhou, Tianjin, and Yantai in China) along the Bohai Sea (DTT assay) (Liu et al., 2018), southeast US (DTT and ascorbate assays) (Fang et al., 2016; Verma et al., 2014), and California (DTT assay) (Charrier et al., 2015). These studies, although limited, generally indicate highly differential profiles of the emission sources for their contribution to OP vs. $PM_{2.5}$ mass. For example, in the study conducted by Yu et al. (2019) at an urban site in Beijing, vehicular emission was responsible for only $\sim \! 10\%$ of PM_{2.5} mass concentrations in summer and fall, but led to more than half of the $PM_{2.5}$ OP measured by the DTT assay. Similarly, the contributions of secondary oxidation, biomass burning, and vehicular emissions in PM2.5 mass for the source apportionment study conducted in southeast US were 58%, 14%, and 12%, respectively, compared to 29%, 35% and 16% contributions in the DTT-based OP (Bates et al., 2015). As DTT activity turned out to be a better predictor of asthma and congestive heart failure in that study,

controlling its sources would be a more effective strategy to prevent the adverse health effects of $PM_{2.5}$ than the mass. Note, most of the OP source apportionment results conducted so far have employed only the chemical OP assays. To the best of our knowledge, we have found only three studies that had used a cellular OP assay to conduct the source apportionment analysis, that too were based on a relatively smaller sample size collected from only a single urban site, i.e., Denver, CO (N = 45 daily samples) (Zhang et al., 2008), Athens, Greece (N = 22 weekly samples) (Taghvaee et al., 2019), and Seoul, Korea (N = 52 daily samples) (Park et al., 2018). Moreover, none of these studies have systematically compared the contribution of various emission sources to the $PM_{2.5}$ mass vs. cellular OP.

Given the dearth of literature on apportioning the emission sources contributing to cellular OP on a relatively large regional scale, this study focuses on the spatiotemporal distribution and source apportionment of macrophage ROS activity of ambient PM2.5 in the Midwestern United States. The study is based on an extensive sampling campaign conducted for a year at five distinct sites - 3 urban, 1 rural and 1 roadside, in the Midwest US. A macrophage ROS assay using rat alveolar macrophages was used for assessing the cellular OP of the ambient PM_{2.5}. In addition, the detailed chemical characterization of the samples was conducted by measuring the concentration of elemental carbon (EC), OC, WSOC, brown carbon (BrnC), water-soluble elements, and inorganic ions. Finally, both the chemical composition and macrophage ROS data were processed by PMF to identify the emission sources contributing to cellular OP. The results were compared with a parallel source apportionment analysis conducted on the PM2.5 mass. Our study presents a comprehensive analysis of the sources of a cellular OP endpoint using a large number of samples collected from a region, which is rather understudied in terms of the ambient PM2.5 pollution and its health

2. Materials and methods

2.1. Reagents

Nitric acid (HNO₃, \leq 70%) was ordered from Avantor sciences (Radnor, PA). Hydrochloric acid (HCl, ACS grade) was bought from EMD Millipore Corporation (Billerica, Ma). We purchased the total organic carbon (TOC) standard (500 ppm, consisting a mixture of hydrochloric acid, potassium hydrogen phthalate, and water) from Aqua Solutions, Inc (Deer Park, TX). Methanol (HPLC grade) was bought from Fisher Scientific (Fair Lawn, NJ). Multi-Element Calibration Standard 3 was bought from PerkinElmer, Inc (Waltham, MA). 2',7'-Dichlorofluorescin diacetate (DCFH-DA, \geq 97%), zymosan, dimethyl formamide, HEPES (\geq 99.5%), sodium chloride (NaCl, \geq 99.5%), potassium chloride (KCl, \geq 99%), calcium chloride (CaCl₂, \geq 96%), dextrose (\geq 99.5%), sodium hydroxide (NaOH, 99.99%), 2-phenylphenol (99%), and sodium nitroprusside dihydrate (\geq 99%) were bought from Sigma-Aldrich Co. (St. Louis, MO).

2.2. PM_{2.5} samples collection and filters extraction

We deployed five high-volume samplers (HiVol, Thermo Anderson, nominal flow rate $1.13~\text{m}^3~\text{min}^{-1}$, $PM_{2.5}$ impactor) at five different locations, three of which can be considered as urban background, one rural and one roadside site. The urban background sites were located in three major cities – Chicago (IL), St. Louis (MO), and Indianapolis (IN). Chicago site (CHI, 41°50′12″ N, 87°37′29″ W) was located on a student dorm in Illinois Institute of Technology (IIT). This site is surrounded by six large parking lots, one parking garage, and a Chicago subway station (Sox-35th) is within 100 m. Also, the freeway I-90 is 400 m away on west side of this site. The sampling site in Indianapolis (IND, 39°46′44″ N, 86°10′38″ W) was in Indiana University–Purdue University Indianapolis campus. This site is also surrounded by several parking garages and parking lots. St. Louis site (STL, 38°39′23″ N 90°11′54″ W) is on

north side of downtown St. Louis. More specifically, this site is at the boundary between residential areas and an industrial zone consisting of various industries (e.g., metal processing, industrial cleaning products, salt manufacturing, pharmaceuticals, and metal recycling, etc.). The distance of freeway I-70 from this site is only 150 m. It is an Ncore (National Core Pollutants) site and has been used in previous regional source apportionment studies based on PM_{2.5} mass (Amato and Hopke, 2012; Lee and Hopke, 2006). Champaign site (CMP, 40°06'58"N, 88°13'31"W) is adjacent to a major road (University Ave.) in the UIUC campus. As shown in a previous research (Wang et al., 2018), this site is impacted by the vehicular emissions in addition to the road-dust resuspension. Besides these sites in urban locations, one sampler was placed in a rural area, Bondville (BON, 40°03'05"N, 88°22'09"W). Other than the secondary sources as reported in a previous study (Kim et al., 2005), agricultural activities from the nearby farmlands seem to be the only major source of emissions at this site. A more detailed description of these sites is provided in our previous study (Yu et al., 2021).

All the samplers started collecting PM2.5 on Tuesday 0:00, and automatically shut down on Friday 0:00. The samples from all the sites were collected on Friday morning, and the samplers were loaded with new pre-baked (at 550 °C) quartz filters (Tissuguartz 2500QAT-UP, Pall life Sciences, Port Washington, NY) at that time. All the filters were weighed both pre- and post-sampling to determine the PM2.5 mass loadings. Prior to each weighing, filters were kept in a constant temperature (24 °C) and humidity room (~50%) for 24 h. After weighing, filters were wrapped in prebaked Aluminum foil and stored in a −20 °C freezer. Our sampling campaign started on 05/22/2018 and completed on 05/31/2019, with a total of 241 samples collected from all the sites: 45 from BON, 44 from CHI, 51 from CMP, 54 from IND, and 47 from STL. More details of sampling are provided in Yu et al. (2021). The sampling period was classified into four seasons - summer (June-August 2018), fall (September-November 2018), winter (December 2018-February 2019) and spring (May 2018 to May 2019).

The macrophage ROS assay was conducted on the water-soluble extracts of ambient $PM_{2.5}$. To prepare the $PM_{2.5}$ water-soluble extract, we cut a circular section (16 mm diameter) from the filter, immersed it in 5 mL of deionized water (DI; Milli-Q; resistivity = $18.2 \text{ M}\Omega/\text{cm}$), and sonicated it for 1 h. After sonication, we removed the fibers or insoluble particles by filtering the extract through a $0.45 \mu m$ syringe filter.

2.3. Cellular ROS measurement

2.3.1. Macrophage cells

Rat macrophage cell line NR8383 was chosen for the cellular OP assay. Incubation of the macrophage cells followed the instructions from the American Type Culture Collection (ATCC) (Landreman et al., 2008). Ham's F-12 K (Kaighn's) medium that contains 1500 mg/L sodium bicarbonate, 2 mM L-glutamine, and 15% of the heat-inactivated fetal bovine serum was used to maintain the cells. Cells were cultured in the plastic petri dishes kept in a humidified incubator at 37 °C and 5% CO₂.

2.3.2. Assay related solutions preparation

 $1\times$ Salts Glucose Medium (SGM) which contains 50 mM HEPES, 100 mM NaCl, 5 mM KCl, 2 mM CaCl₂, and 5 mM dextrose, was made by dissolving 5.958 g HEPES, 2.922 g NaCl, 0.1864 g KCl, 0.1470 g CaCl₂, and 0.4504 g dextrose in 500 mL of DI. The solution was further filtersterilized by a sterile disposable vacuum filter unit (Fisherbrand). 10 folds concentrated SGM (10 \times SGM) was also prepared in the same manner with all components in 10 times concentrations as used in 1 \times SGM. To make 45 mM DCFH-DA solution, 21.8 mg DCFH-DA was dissolved in 1 mL dimethylformamide. From this stock DCFH-DA solution, 30 μ L was aliquoted into several 1.5 mL vials (30 vials, each containing 30 μ L DCFH-DA), and all of them were stored in a -20° C freezer. This stock DCFH-DA solution was serially diluted with SGM, to make a working solution (400 μ M). In the first dilution, we mixed 25 μ L of

45 mM DCFH-DA with 225 μ L 1 \times SGM to obtain 4.5 mM DCFH-DA. 135 μL of this DCFH-DA was again mixed with 590 μL 10 \times SGM and 775 μ L 1 \times SGM to obtain the DCFH-DA working solution. Since, none of the exposure samples, i.e., negative control (DI), ambient PM_{2.5} extract, or positive control contained any nutrients, this working solution served as a medium to maintain a constant nutrient concentration in all the exposure vials. We chose zymosan (a glucan synthesized by yeast) as the positive control for each macrophage ROS experiment and also to normalize our results, thus making them comparable with other PM_{2.5} OP studies using macrophage ROS assay (Brehmer et al., 2020; Taghvaee et al., 2019; Zhang et al., 2008). The unit of mass-normalized OP and volume-normalized OP were expressed as μg of zymosan units/mg of PM_{2.5} and µg of zymosan units/m³ of air, respectively, which are consistent with previously studies based on macrophage ROS assay (Al Hanai et al., 2019; Park et al., 2018). To prepare the positive control, we added 10 mg zymosan in 10 mL DI. After mixing the solution on a vortex mixer for at least 1 min, we transferred 2.56 mL solution into a 15 mL centrifuge vial and added 7.44 mL DI to make 0.256 mg/mL zymosan stock. The zymosan stock was kept in a refrigerator and was vortexed for 1 min prior to any use. The final exposure concentration of zymosan was 0.1 mg/mL. All the water-soluble PM_{2.5} extracts were diluted to <64 µg PM_{2.5} mass/mL DI, so that when they were mixed with cells and DCFH-DA, the final $PM_{2.5}$ concentration became 25 μg $PM_{2.5}$ mass/mL or lower for all exposure experiments. The reason for controlling the PM concentration in the exposure vials is discussed in the next Section.

2.3.3. Macrophage ROS assay

This assay is adapted from Landreman et al. (2008) but with a few modifications so that the fluorescence can be measured by our bench-top spectrofluorometer (RF-5301 pc, Shimadzu Co., Japan), instead of a plate reader in the original method. Floating cells were harvested from the plastic culture plates, and cell density was counted with a hemocytometer. Subsequently, cell solutions were centrifuged (Sorvall Legend X1R Centrifuge, Thermo Scientific, Germany) at the rate of 1000 rpm for 10 min. After spinning the cells down, the supernatant was removed by a glass Pasteur pipette connected to a vacuum valve. A calculated volume of 1X SGM was mixed with the cell pellet to make the final cell concentration as 2000 $\#/\mu L$. Finally, 39 μL of the DCFH-DA working solution was mixed with 177 μL cell suspension and 138 μL of either of DI (negative control) or PM_{2.5} extract or positive control (zymosan) in a 1.5 mL vial. All the samples, i.e., negative control, PM_{2.5} extracts, and positive control were analyzed in triplicates. All these vials were then kept in an incubator. After 2.5 h of incubation, 30 μL of the mixture was taken from each vial and diluted with 2000 µL DI, before measuring the fluorescence at 488/530 nm. The consistency of the measurement protocol was assessed by calculating the ratio of fluorescence caused by positive control (zymosan) to negative control (cells treated with only glucose medium and DCFH-DA). The average (\pm 1 σ) ratio from all our positive control measurements was 3.7 \pm 0.5 (N = 46), which was very close to the value (4.1) reported by Landreman et al. (2008), ensuring the consistency of our measurements.

Since the cellular ROS response can get saturated if the cells are exposed to a very high concentration of the toxic substance (Rodhe et al., 2015; Stoiber et al., 2013), it is important to choose an appropriate concentration of the PM_{2.5} extracts for cellular exposure to avoid underestimation of the cellular OP. Therefore, we exposed the cells to different concentrations (0, 13.5, 27, 50, and 108 μ g/mL) of a randomly chosen PM_{2.5} extract (CHI05/29/2018, a sample collected from Chicago during 05/29/2018–05/31/2018), with a goal to obtain a linear range for the PM_{2.5} concentration-cellular ROS response. As shown in Fig. S1 (SI), the ROS response for this sample remained linear below 27 μ g/mL, above which it starts plateauing. This linear range of the ROS response with the concentration of PM_{2.5} extracts was further confirmed by 7 more samples chosen randomly and extracted in water at three concentrations (0, 15, and 30 μ g/mL) (Fig. S1). Based on these tests, we ensured to keep the concentrations of PM_{2.5} extracts in all of our

exposure vials below or equal to 25 µg/mL.

Moreover, since our adapted method used a benchtop spectrofluorometer instead of the plate reader to measure the fluorescence caused by cellular ROS, to ensure there is no bias caused by this difference, we measured the macrophage ROS activity of 10 ambient PM_{2.5} extracts by both methods. As shown in Fig. S2 (SI), there is an excellent agreement between these two methods with a coefficient of determination (R^2) = 0.97 and a slope close to 1, indicating the efficacy of our spectrofluorometric method to measure the ROS generated by the cells undergoing oxidative stress.

2.4. Chemical composition analysis

The concentration of EC and OC was determined based on the National Institute for Occupational Safety and Health (NIOSH) protocol 5040 (Birch and Cary, 1996). We punched a small fraction (1 \times 1 cm²) from each filter and directly analyzed its EC/OC content with a thermal/optical transmittance (TOT) analyzer (Sunset Laboratory). For measuring the concentration of WSOC, we transferred 1.5 mL of the diluted water-soluble PM_{2.5} extracts to 30 mL glass bottles and further diluted it with DI to 25 mL. Prior to the transfer, the glass bottles were rinsed with DI, dried in the fume hood and then baked in an oven at 550 °C for 24 h to remove any organic residues. The diluted PM_{2.5} samples were acidified to pH <2 by adding 25 μL of HCl to convert CO₃²⁻ and HCO₃⁻ to CO₂. The concentration of WSOC in these acidified PM_{2.5} extracts were then measured by a TOC analyzer (TOC-V_{CPH}, Shimadzu Co., Japan). The instrument was calibrated by measuring TOC standards of different concentrations (0, 1, 1.25, 1.67, 2.5, and 5 ppm) before measuring each batch (consisting of ~ 20 PM_{2.5} samples). The measurement of BrnC was based on the protocol used in several past studies (Cheng et al., 2016; Hecobian et al., 2010; Kirillova et al., 2016; Liu et al., 2013; Wu et al., 2019; Zhu et al., 2018). The BrnC quantification was derived from Beer's Law:

$$A_{\lambda} = -log_{10}\left(\frac{I}{I_0}\right) = l \cdot \sum_{i} C_i \cdot \varepsilon_i = l \cdot Abs_l$$

Where A_{λ} is the measured absorption, I and I_0 are the intensity of transmitted and incident light, respectively, C_i is the concentration of the light-absorbing compound i in the solution, ϵ_i is the mass absorption efficiency of compound i, l is the absorbing path length, Abs_l is the BrnC's absorption coefficient in the solution. To express the absorption coefficient into equivalent ambient units, the above equation can be written as:

$$Abs365 = (A365 - A700) \frac{C_a}{C_l \cdot l} ln \overline{\underline{fo}} (10)$$

Where A_{365} and A_{700} are the absorbance of $PM_{2.5}$ water extract (10 μg $PM_{2.5}$ per mL of DI) at 365 and 700 nm. C_a is the concentration of $PM_{2.5}$ in the air ($\mu g/m^3$). C_l is the concentration of $PM_{2.5}$ in the extract (10 $\mu g/mL$). The absorbing path length (l) was 1 m in our experiments. The absorption coefficient (Abs₃₆₅) in unit of Mm^{-1} is equivalent to the representation of BrnC in ambient mass concentration. An online spectrophotometer (Ocean Optics, Inc., Dunedin, FL) coupled to a liquid waveguide capillary cell (LWCC-M-100; World Precision Instruments, Inc., Sarasota, FL) was used to measure the absorbance of $PM_{2.5}$ extracts at both 365 and 700 nm wavelengths.

NexION 300X inductively coupled plasma mass spectrometer (ICP-MS; Perkin Elmer, Waltham, MA) was used to analyze the concentrations of 14 elements (Li, Al, K, V, Cr, Ni, As, Se, Ba, Pb, Zn, Cu, Fe and Mn) in the water-soluble $PM_{2.5}$ extracts. A multi-element calibration standard with equal concentrations of each element (10 ppm each) was used for the calibration. To build the calibration curves, we prepared a concentration gradient (0, 5, 10, 20, 40, 80 ppb) for all measured elements by diluting this standard solution.

The concentrations of sulfate (SO₄²-) and nitrate (NO₃⁻) in the water-

soluble PM_{2.5} extracts were determined via a Dionex ICS-2100 ion chromatography system which is equipped with a Dionex IonPac AS18 column. The method for the water-soluble ammonium (NH₄⁺) measurement was adapted from Kanda (1995). Briefly, we mixed the diluted water-soluble PM_{2.5} extract (5 mL) with 0.8% sodium hypochlorite (0.05 mL), 40 g/L o-phenylphenol (OPP) (0.1 mL), and 400 g/L trisodium citrate (1 mL). After 5 min, 0.5 g/L sodium nitroprusside (NaNP) (0.1 mL), which was prepared by adding sodium nitroprusside into 3 N NaOH solution, was transferred into the mixture. The sample was then incubated at 40 °C for 15 min. In the presence of NaNP, OPP reacts with NH₄⁺ and forms a blue indophenolic compound. The product was quantified by a spectrophotometer (UV-2401PC, Shimadzu Corporation, Japan) by measuring the absorbance at 670 nm wavelength. To calibrate NH₄⁺ measurement method, we made standard solutions of ammonium sulfate ((NH₄)₂SO₄) ranging from 0 to 80 μM NH₄⁺ and analyzed them following the same protocol. A typical standard calibration curve for (NH₄)₂SO₄ is shown in Fig. S3 of SI.

2.5. OP Source apportionment using PMF and other statistical analysis

PMF is based on the receptor modeling technique (Paatero and Tapper, 1993; Sun et al., 2020). The receptor model takes the advantage of unique species profile in each source to solve the mass balance between chemical composition of the collected samples and the source emission profile. The equation of the receptor model is described below:

$$x_{ij} = \sum_{k=1}^{p} g_{ik} f_{kj} + e_{ij}$$

Where x_{ij} represents the concentration of species j in sample number i; p is the total number of emission sources; g_{ik} denotes the contribution factor of source k in sample i; f_{kj} is the source profile of source k for species j; and e_{ij} is the residual for each x_{ij} . Derived from the above equation, PMF reduces the objective function Q:

$$Q = \sum_{i=1}^{n} \sum_{j=1}^{m} \left[\frac{x_{ij} - \sum_{k=1}^{p} g_{ik} f_{kj}}{u_{ij}} \right]^{2}$$

Where u_{ij} is the uncertainty for each x_{ij} . Majority (99%) of our ambient data was above the method detection limit (MDL), and for those below MDL, the concentrations were set to 1/3 of MDL with corresponding uncertainties replaced by 5/6 of MDL (Kundu and Stone, 2014). The uncertainties for each chemical species used in PMF were the overall uncertainties obtained by propagating the uncertainties at each step starting from filter collection to analysis. The analytical uncertainties were obtained by analyzing the standards (e.g., zymosan for macrophage ROS, sucrose solution for OC, TOC standard for WSOC, multi-element calibration standard for elements, NH₄NO₃ for NO₃, and (NH₄)₂SO₄) for SO₄²⁻ and NH₄⁺) or the same ambient sample analyzed multiple (N > 6) times (for BrnC and EC) and calculating the standard deviation from the measurement. The missing data were replaced with the median values for that component, and an uncertainty of 400% were assigned for those values (Verma et al., 2014). Separate PMF runs were conducted for cellular OP and PM2.5 mass, while choosing them as the total variable for apportioning the contribution of various factors to OP and $PM_{2.5}$ mass, respectively. For the base runs (N = 20), a seed of 15 was chosen and the model was executed for various numbers of the factors (4-9). The correlation among individual factors was tested by G-space plots. The solution space of these plots was filled by the contribution values indicating the independence of different factors.

Seasonal and spatial OP variations were assessed by analysis of variance (ANOVA) using SPSS 27. A correlation analysis (Pearson's r) between various parameters such as OP vs. $PM_{2.5}$ components, OP at various sites and intercorrelation among various $PM_{2.5}$ components, was conducted using SPSS 27. The correlations with P < 0.05 (irrespective of

r) were considered significant, while those with $r{\geq}0.6$ and P<0.05 were considered strong. The spatial heterogeneity of cellular OP was also assessed by determining coefficient of divergence (COD), using the following equation:

COD =
$$\sqrt{\frac{1}{N} \sum_{i=1}^{N} \left[\frac{c_{ij} - c_{ik}}{c_{ij} + c_{ik}} \right]^2}$$

Where c_{ij} and c_{jk} are the cellular OP at sampling site j and k, N is the number of samples. COD varies from 0 to 1, with lower values (<0.5) indicating spatial homogeneity, while higher values (>0.5) indicate spatial heterogeneity.

3. Results and discussions

3.1. Macrophage ROS results overview

Fig. 1 shows time-series of the volume-normalized (OP_v) and mass-normalized cellular OP (OP_m) of the water-soluble $PM_{2.5}$ extracts. The ranges of the water-soluble OP_v and OP_m observed in our study were $0.73-50.77~\mu g$ of zymosan units/m³ and $115-4253~\mu g$ of zymosan units/mg PM, respectively. These results are in the typical range of macrophage OP reported for the ambient PM measured at several locations, such as Los Angeles (OP_v : $0.3-110~\mu g$ of zymosan units/m³; OP_m : $50-18,000~\mu g$ of zymosan units/mg PM) (Cheung et al., 2012; Hu et al., 2008; Verma et al., 2009a, 2009b), Lahore (Pakistan) (OP_m : $700-14000~\mu g$ of zymosan units/mg PM) (Shafer et al., 2010), Baghdad

(Iraq) (OP $_{\rm m}$: 20–180 µg of zymosan units/mg PM) (Hamad et al., 2016), and Tehran (Iran) (OP $_{\rm m}$: 1500–5500 µg of zymosan units/mg PM) (Al Hanai et al., 2019). As shown in Fig. 1, water-soluble OP $_{\rm v}$ and OP $_{\rm m}$ seem to have a similar spatiotemporal trend with their peaks occurring in summer. It indicates only a marginal role of PM $_{2.5}$ mass in controlling the spatiotemporal distribution of the cellular OP.

3.2. Spatial-temporal variation

The seasonal averages of water-soluble OP_v and OP_m at five sites are shown in Fig. 2. Summer had the highest mean water-soluble OP_v and OP_m , while the mean water-soluble OP_v and OP_m were usually the lowest in winter. The seasonal variation profiles of cellular OP in our study are similar to those in Denver, CO (Zhang et al., 2008), Los Angeles, CA (Cheung et al., 2012), and Athens, Greece (Taghvaee et al., 2019), all of which reported the highest activity in summer and lowest in winter. Among the five locations, only CMP had an insignificant seasonal variation in the water-soluble OP (P > 0.05 for both OP_v and OP_m , F-value for $OP_v = 2.29$ and $OP_m = 1.42$ for the one-way ANOVA test; Table S1 and S2). On the other hand, BON had the strongest seasonal variability (P < 0.01 for OP_v and OP_m , F-value for $OP_v = 9.73$ and $OP_m = 7.95$). Given that BON is a rural site, the strong seasonality in water-soluble OP there is possibly related to the agricultural activities.

Fig. 2 also suggests that the water-soluble OP in the Midwest US is spatially homogenous. We found no significant differences in the mean water-soluble OP_v (F<2.03, P>0.12; Table S3) and OP_m (F<2.61, P>0.05) at various sites across different seasons (except spring; P=0.04). Interestingly, the cellular OP (both mass and volume-

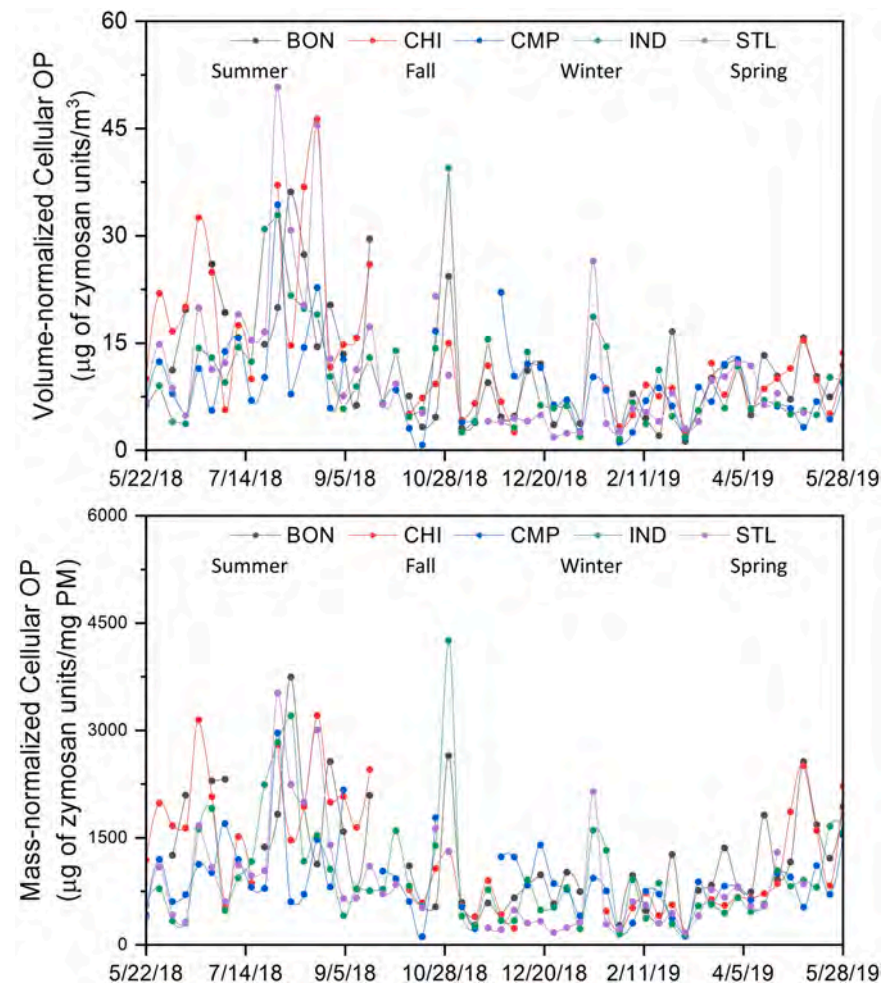


Fig. 1. Time series of volume-(top) and mass-(bottom) normalized water-soluble cellular OP at the sampling sites.

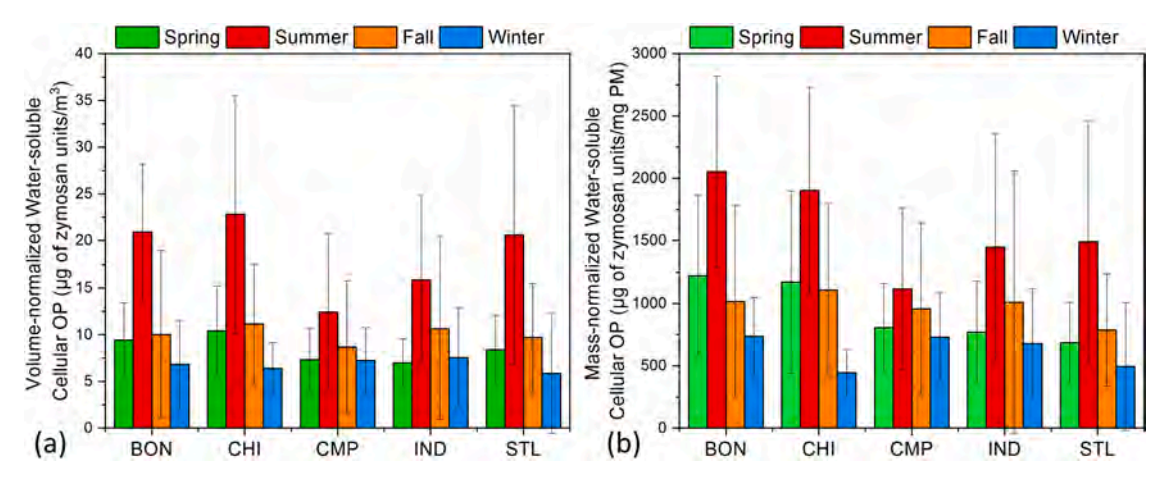


Fig. 2. Seasonal averages of volume-(left) and mass-(right) normalized water-soluble cellular OP at the sampling sites. (Error bars denote one standard deviation from the mean.).

normalized) at BON were comparable (or even slightly higher) to other urban sites. Garcia et al. (2016) assessed the health risk of $PM_{2.5}$ to elderly residents in urban and rural California. The RRs of $PM_{2.5}$ -related cardiovascular disease, cardiopulmonary disease, and mortality in rural areas were higher [e.g., RR for mortality = 1.128 (95% CI: 1.098, 1.162)] than in urban areas [0.988(95% CI: 0.978,1.002)]. Our study, supporting their results highlights the importance of assessing the air quality and its health impacts in rural regions as well.

To further quantify the spatial variability in PM_{2.5} water-soluble OP_v and OP_m, we calculated the CODs and correlation coefficients (Pearson's r) for different site pairs. The CODs for water-soluble OP_v and OP_m were within the range of 0.25–0.37 (Table 1), further confirming a spatially homogenous profile for both cellular OP in the Midwest US. With the exception for the pair CMP-BON, all of the correlation coefficients were highly significant (P < 0.01), and many of these were quite strong ($r \geq 0.6$). It implies that there are many common sources impacting the macrophage ROS activity at most of these sites.

3.3. Correlation of OP with PM_{2.5} chemical components

To investigate the specific constituents that could influence the spatiotemporal distribution of water-soluble OP, we correlated the volume-normalized macrophage ROS activity with the ambient concentrations of measured PM_{2.5} components in Table 2. Here, we have composited all the data without any segregation of different seasons. We have defined the correlations as significant if P < 0.05, and among the significant correlations, those with Pearson's $r \ge 0.60$ are defined as strong correlations. The correlations of PM_{2.5} mass concentration with

water-soluble $\mathrm{OP_{v}}$ were weak, with only two sites (BON and CMP) showing some significant correlations (r=0.42 and P<0.05 at BON, r=0.39 and P<0.05 at CMP). Components such as Ba, Se, Ni, Cr, V, K, Zn, EC, BrnC, $\mathrm{SO_4}^2$ -, $\mathrm{NO_3}$ -, $\mathrm{NH_4}^+$, etc., were poorly correlated with the water-soluble cellular OP. However, significant correlations (P<0.05) with water-soluble OP were observed for Al, Pb, Mn, Fe, As and WSOC. Among all measured components only Fe and WSOC were strongly ($r\ge0.60$, P<0.05 in many cases) correlated with the water-soluble OP at all the sites.

Next, we segregated these correlations in different seasons (Tables S4–S8). In the season-segregated correlation, more PM components started showing some strong correlations, which was expected given the seasonality of different emission sources with unique chemical composition profiles. Generally, the correlations of the measured chemical components were better in fall and winter seasons than in summer and spring. At BON, many elements such as Li, Al, K, Mn, Zn, Pb, As, and Fe, were correlated with the macrophage ROS activity, particularly during the fall and winter. A subset of these species (Li, K, Mn, Pb, As and Fe) showed good correlations with the ROS at CMP as well. However, the correlations were stronger during fall than winter.

At CHI, a few metals, such as Al, V, Cu, Pb, and Fe, were strongly correlated with the macrophage ROS again during the fall season. IND site also showed some significant correlations with Al, Cr, Mn, Pb, and Se during fall. Some of these elements (Cr, Cu, Pb and Fe) were correlated with ROS at STL site as well but only during the winter season. After Fe, Pb showed the most consistent correlation with ROS among all the metals; it was correlated with ROS at all the sites during fall or winter. There have been several studies showing the correlation of V and Ni with

Table 1 Spatial heterogeneity of cellular OP_v and OP_m assessed by coefficient of divergence (COD) and Pearson's r for different site pairs.

			•					•		
Coefficient of	Divergence (COI	D)								
	OP_v					OP_m				
	BON	CHI	CMP	IND	STL	BON	CHI	CMP	IND	STL
BON	-	0.27	0.36	0.3	0.32	-	0.25	0.34	0.33	0.37
CHI		_	0.35	0.29	0.27		-	0.33	0.32	0.29
CMP			_	0.28	0.33			-	0.31	0.34
IND				-	0.27				_	0.26
STL					_					-
Pearson's r										
	OP_v	OP_m								
	BON	CHI	CMP	IND	STL	BON	CHI	CMP	IND	STL
BON	_	0.59 *	0.26	0.54 *	0.50 *	_	0.58 *	0.22	0.56 *	0.47 *
CHI		_	0.60 *	0.57 *	0.76 *		_	0.51 *	0.41 *	0.69 *
CMP			_	0.61 *	0.71 *			_	0.38 *	0.53 *
IND				_	0.64 *				_	0.66 *
STL					_					_

Note: * indicates significant correlations (P < 0.05).

 Table 2

 Correlations of water-soluble $PM_{2.5}$ cellular OP with $PM_{2.5}$ components and mass concentration (Pearson's r).

	OP_{v}	OP _v					OP_m					
	BON	CHI	CMP	IND	STL	BON	CHI	CMP	IND	STL		
Fe	0.79 *	0.78 *	0.62 *	0.60 *	0.73 *	0.75 *	0.77 *	0.44 *	0.61 *	0.76 *		
WSOC	0.74 *	0.81 *	0.58 *	0.51 *	0.61 *	0.56 *	0.78 *	0.44 *	0.47 *	0.60 *		
OC	0.68 *	0.69 *	0.52 *	0.42 *	0.50 *	0.49 *	0.68 *	0.33 *	0.40 *	0.44 *		
Al	0.59 *	0.51 *	0.37 *	0.27 *	0.34 *	0.52 *	0.50 *	0.17	0.43 *	0.39 *		
Pb	0.43 *	0.60 *	0.63 *	0.63 *	0.23	0.40 *	0.57 *	0.49 *	0.69 *	0.21		
Mn	0.54 *	0.25	0.32 *	0.66 *	0.39 *	0.44 *	0.23	0.14	0.68 *	0.37 *		
As	0.45 *	0.50 *	0.54 *	0.27 *	0.18	0.34 *	0.44 *	0.41 *	0.27 *	0.15		
Cu	0.60 *	0.27	0.35 *	0.25	0.16	0.48 *	0.33 *	0.31 *	0.27 *	0.13		
Li	0.50 *	0.14	0.42 *	0.34 *	0.15	0.32 *	0.16	0.26	0.41 * *	0.15		
Ba	0.15	0.23	0.45 *	0.14	0.07	0.04	0.22	0.35 *	0.19	-0.05		
Se	0.39 *	0.36 *	0.28	0.22	0.08	0.26	0.43 *	0.09	0.31 *	0.01		
Ni	0.33 *	0.30	0.41 *	-0.11	0.49 *	0.27	0.28	0.24	-0.09	0.45 *		
Cr	0.57 *	0.17	0.44 *	0.33 *	0.13	0.51 *	0.21	0.23	0.39 *	0.13		
V	0.44 *	0.30 *	0.31 *	0.15	0.06	0.27	0.41 *	0.15	0.26	0.07		
K	0.64 *	0.25	0.48 *	0.13	0.03	0.54 *	0.23	0.34 *	0.21	-0.04		
BrnC	0.20	0.12	0.30 *	0.05	0.08	-0.08	0.04	0.05	0.03	-0.06		
Zn	0.35 *	0.22	0.18	0.14	-0.02	0.24	0.23	0.06	0.21	-0.06		
EC	0.18	0.16	0.17	0.02	0.04	-0.03	0.13	0.02	-0.01	-0.07		
SO_4^{2-}	0.36 *	0.20	0.23	0.16	0.24	0.15	0.29	0.05	0.26	0.29		
NO ₃	-0.20	-0.30 *	-0.01	-0.15	-0.28	-0.40 *	-0.32 *	-0.20	-0.13	-0.27		
NH_4^+	-0.04	-0.24	0.12	-0.05	-0.12	-0.29	-0.34 *	-0.09	-0.11	-0.09		
Mass	0.42 *	0.05	0.39 *	0.12	0.16	_	_	_	_	_		

^{1. *} indicates significant correlations (i.e. P < 0.05). Among these significant correlations, those with r > 0.60 are shown in bold.

the macrophage ROS, particularly at the sites impacted by ship emissions (Al Hanai et al., 2019; Hamad et al., 2016; Hu et al., 2008). However, in our study, other than at BON (winter: r=0.73 for V; fall: r=0.62 for Ni) and CHI (r>0.6 for V in both spring and fall), we didn't see any significant correlation of these species with the macrophage ROS, even at STL, which is known for the significant activities associated with the movement of shipping vessels.

Inorganic ions such as SO_4^{-2} , NH_4^+ and NO_3^- also showed some intermittent correlation with the macrophage ROS during fall and winter seasons. Particularly, both NH_4^+ and NO_3^- are strongly correlated

with the ROS during winter, probably due to the predominant formation of $\mathrm{NH_4NO_3}$ in cold weather. Although, $\mathrm{NH_4NO_3}$ does not play a direct role in the macrophage ROS generation (Salana et al., 2021), we anticipate that its formation mechanism is probably associated with the formation of other redox-active species [e.g. secondary organic aerosol (SOA)] responsible for the ROS generation. Further mechanistic studies will be required to explore the cause of this correlation. It is interesting that Fe and WSOC were correlated with the macrophage ROS in almost all seasons at most sites (with few exceptions) – a pattern consistent with the combined correlations shown in Table 1.

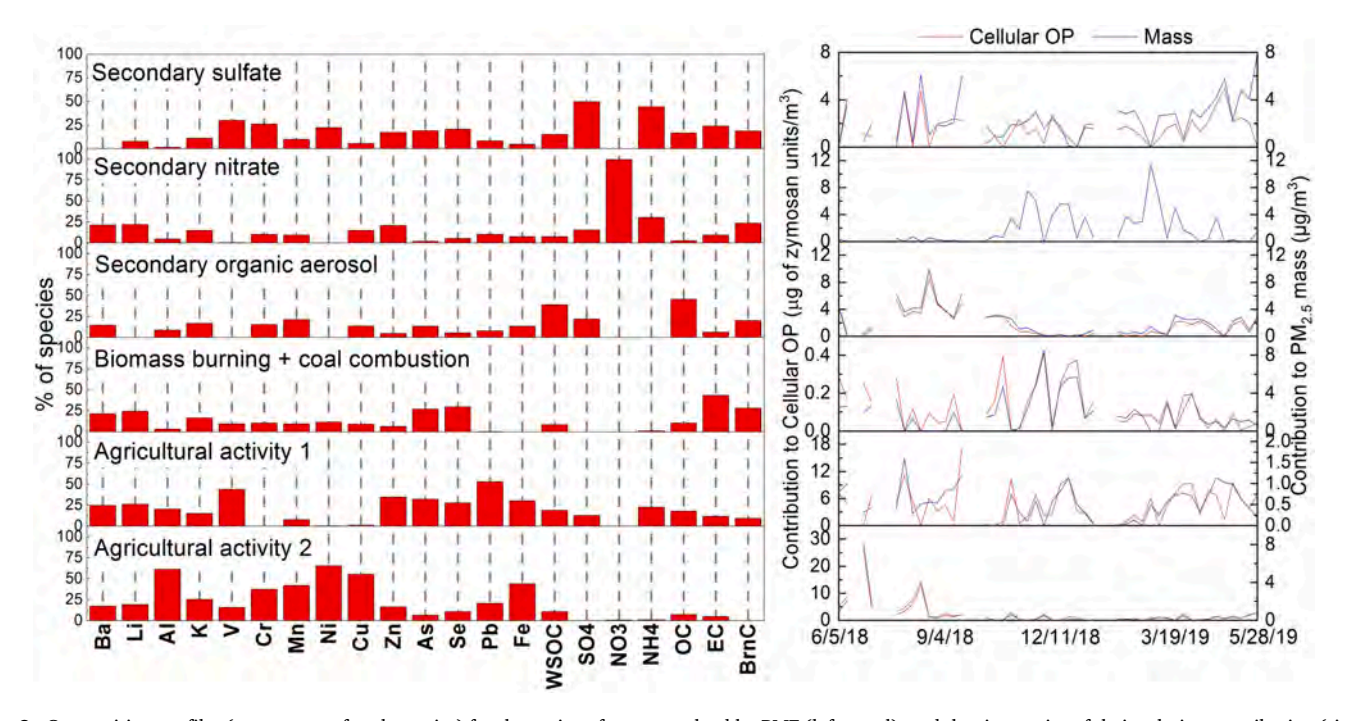


Fig. 3. Composition profiles (percentage of each species) for the various factors resolved by PMF (left panel), and the time series of their relative contribution (right panel) at BON. Composition profiles for the PMF based on both PM_{2.5} mass and cellular OP were almost similar.

^{2.} Since several elements (Al, K, Cr, Cu, Ba) were abnormally elevated (up to 100 times) in the week of July 4th (Independence Day celebration), we removed this week's sample (07/03/2018–07/06/2018) from our regression analysis to avoid any bias caused by this episodic event.

3.4. Source contributions to mass and cellular OP_v

3.4.1. Source identification

To quantify the contribution of different emission sources to cellular OP_v , we conducted a source apportionment analysis using PMF. Figs. 3–7 show the identified sources' profiles at five different sites and the time series of their contributions to cellular OP_v and $PM_{2.5}$ mass. Many common sources such as SOA, secondary sulfate, secondary nitrate, and biomass burning and coal combustion were found at all the five sites, while emissions from agricultural activities, industries, parking, shipping activities, vehicles, and dust were found at the specific sites. To further support the PMF analysis, a detailed correlation matrix of all the $PM_{2.5}$ measured species and OP is also shown in Tables S9-S13 of SI.

The seasonal profile of secondary sulfate was same at all five sites, with its activity being slightly higher in spring and summer, and lower in winter and fall. This trend could be attributed to the photochemical oxidation more prevalent in summer than winter (Duan et al., 2019; Wang et al., 2016). The secondary nitrate was identified based on the concentration of NO_3 , and NH_4 , and this source mostly prevailed in winter, which is consistent with the reported seasonal variation of secondary nitrate in the Midwest US (Kim et al., 2005; Kundu and Stone, 2014; Lee and Hopke, 2006). The formation of secondary nitrate in winter is likely due to prevailing N_2O_5 heterogeneous hydrolysis at nighttime and the partitioning to aerosol phase favored by lower temperatures during winter, as indicated in previous studies (L. Liu et al., 2020; Q.Y. Liu et al., 2020; Wang et al., 2018; Ying, 2011).

We couldn't separate biomass burning from the coal combustion, which were identified based on the mixture of species such as K, As, Se, EC, WSOC, and BrnC. Therefore, this source is categorized as biomass burning + coal combustion, and it was also present at all the sites. K and BrnC are commonly used as markers of biomass burning (Lack et al., 2012; Li et al., 2003a, 2003b), while As and Se are both emitted from coal combustion (Galbreath and Zygarlicke, 2004; Huggins et al., 2007; Reff et al., 2009; Yudovich and Ketris, 2005; Zielinski et al., 2007). BON is ~12 km away from the Abbott Power Plant, which uses natural gas (77%), and coal (23%) to generate electricity. The distance of the CMP to Abbott Power Plant is only 3 km. According to Indiana public media,

the Indiana state still operates 16 coal-fired power plants (Legan, 2020). The Meramec Power Plant is less than 40 km away from STL, and there are several (at least four) coal-fired power plants within 150 km radius of both STL and CHI sites. The reported OC/EC from the coal combustion ranged from 0.8 to 2 (Bond et al., 2004; Chow et al., 2010). The reported mean OC/EC ratios in biomass burning aerosols have larger variation with values varying from 2.8 to 26.2 (Yan et al., 2008; Zhang et al., 2013). In our study, the OC/EC ratios of this mixed source, "biomass burning + coal combustion" at different sites are within or near this range (2.6 at BON, 15.3 at CHI, 10.2 at CMP, 9.6 at IND, and 9.2 at STL). The vehicular emissions, which was identified based on EC concentration and low OC/EC ratio, was also present in all urban sites (OC/EC=1.66, 1.49, 0.12, and 1.72 in CHI, CMP, IND, and STL, respectively).

The SOA source, which was characterized by WSOC (Zhang et al., 2012) and high OC/EC ratio (OC/EC=78.23, 32.21, 46.86, 19.96, and 9.70 in BON, CHI, CMP, IND, and STL, respectively), clearly showed higher activity in summer than winter due to prevalent photochemical formation of SOA in warmer months (Dai et al., 2019). In addition to WSOC, this source is rich in Fe and Pb at all urban sites (CHI, CMP, IND, and STL). It has been known that Fe forms complexes with various atmospheric organic compounds, such as humic-like substances (HULIS) (Wei et al., 2019), oxalate (Tapparo et al., 2020), malonate (Wang et al., 2010), etc. Paris and Desboeufs (2013) systemically investigated the impact of Fe-chelating organic compounds on Fe solubility. The concentrations of oxalate, malonate, and humic acid (an analog of HULIS) were positively associated with dissolved Fe(II). Similar to Fe, Pb is also known to form strong complexes with organic compounds (Al-Masri et al., 2006; Sauve et al., 1998; Weng et al., 2002). Thus, a high concentration of these metals in this source is probably a result of their dissolution due to complexation.

In addition to these common sources, there are also some local sources which are pertinent to the specific sites. For example, suspended dust in CHI and CMP, parking emissions in CHI, CMP and IND, agricultural activities in BON, and shipping and industrial emissions in STL. CMP is located on the roof of a parking deck, while both CHI and IND are surrounded by many parking lots and parking decks. Parking emissions were characterized by abundant Cu, which is a marker of brake wear

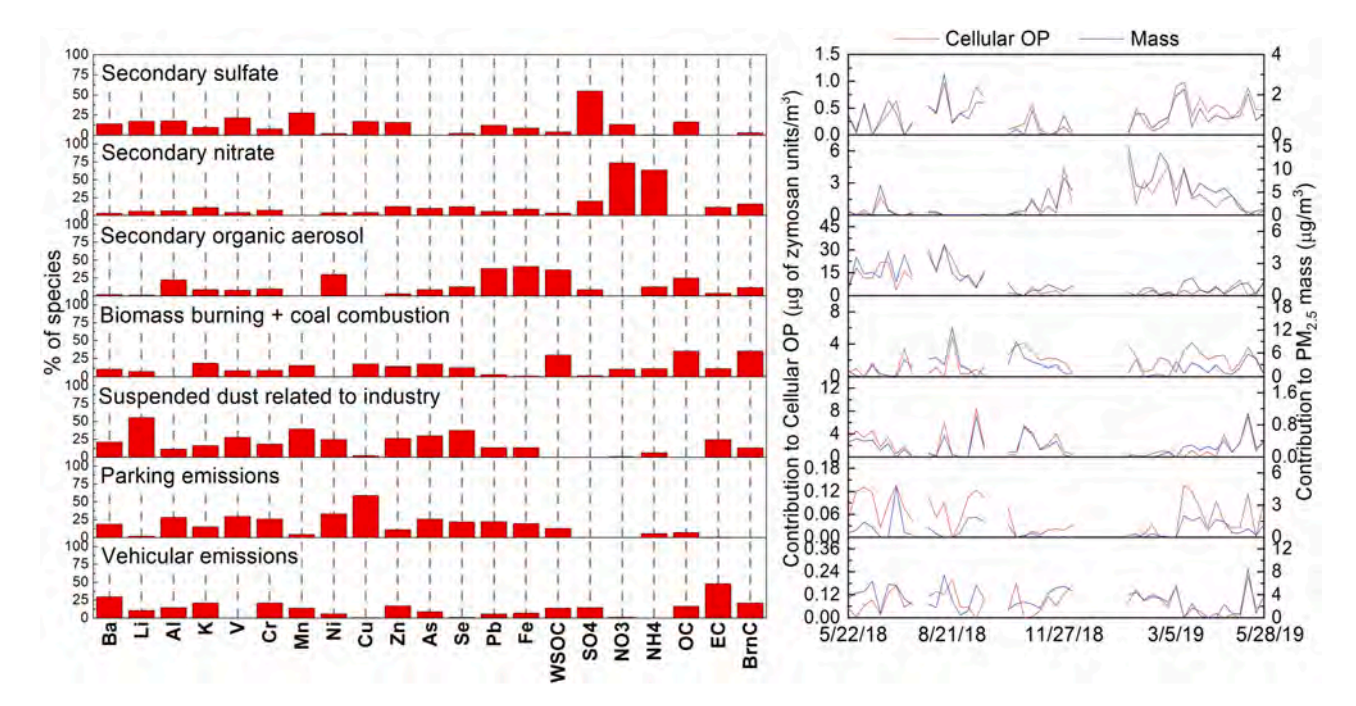


Fig. 4. Composition profiles (percentage of each species) for the various factors resolved by PMF (left panel), and the time series of their relative contribution (right panel) at CHI. Composition profiles for the PMF based on both PM_{2.5} mass and cellular OP were almost similar.

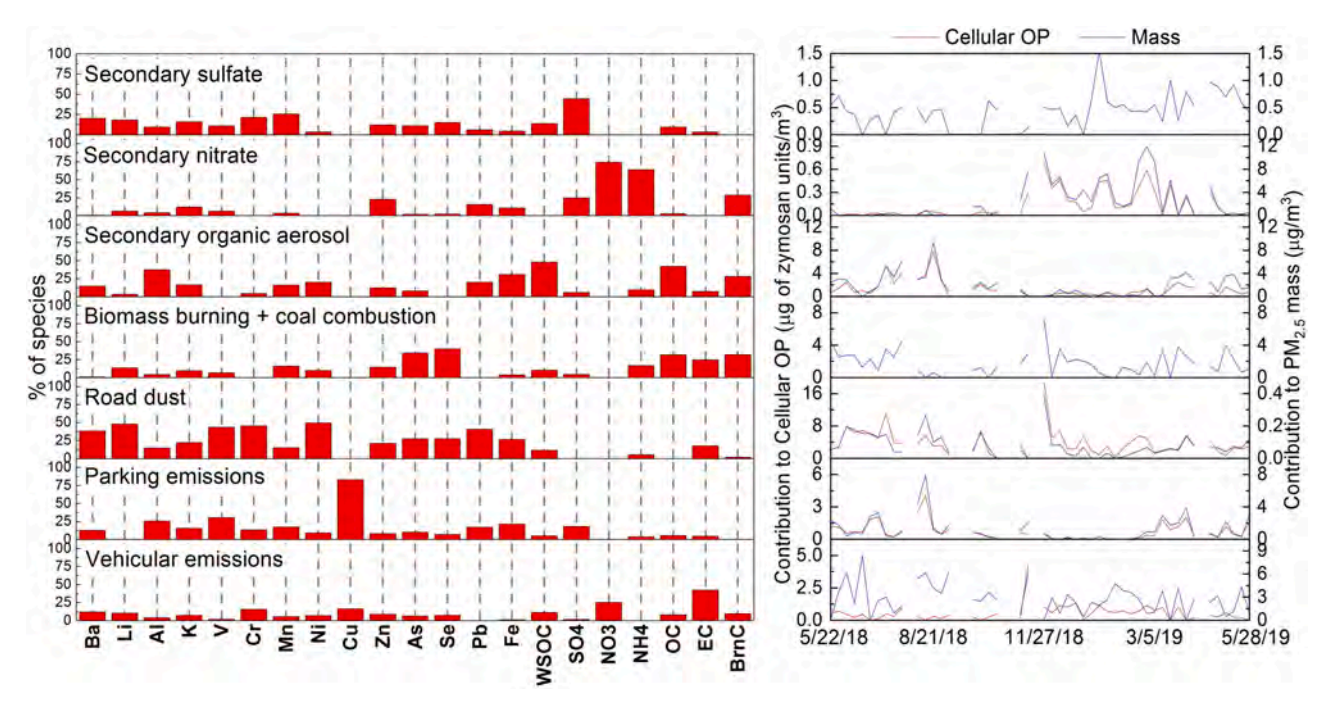


Fig. 5. Composition profiles (percentage of each species) for the various factors resolved by PMF (left panel), and the time series of their relative contribution (right panel) at CMP. Composition profiles for the PMF based on both PM_{2.5} mass and cellular OP were almost similar.

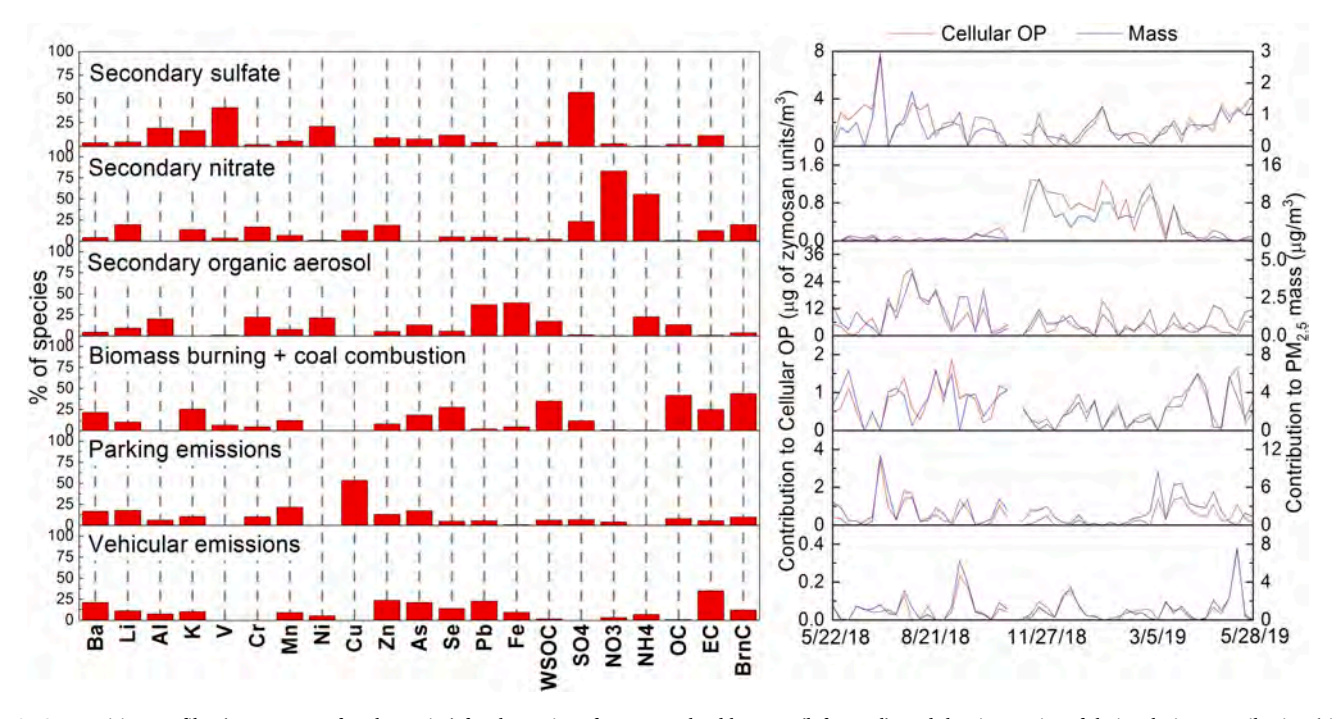


Fig. 6. Composition profiles (percentage of each species) for the various factors resolved by PMF (left panel), and the time series of their relative contribution (right panel) at IND. Composition profiles for the PMF based on both PM_{2.5} mass and cellular OP were almost similar.

(Grigoratos and Martini, 2015). Dust, which was present in CHI, CMP, and IND, was characterized by the abundance of crustal elements (i.e., Al, K, Fe) (Apeagyei et al., 2011; Reff et al., 2009; Silva et al., 2000), and was generally more prevalent in summer than winter, probably due to more construction activities in summer and precipitation caused by snow/rain in the winter. Suspended dust at CHI is rich in several elements, e.g., Li, Mn, Zn, and Ni, which are most likely linked to several local batteries manufacturers, metal recycling and plating industries, e.g., NanoGraf Corporation, Tripp Lite, Sanchem, Inc, Sims Metal, etc. All

these factories are less than 10 km away from this site, probably contributing to the suspended dust in CHI. The road dust at CMP was rich in Ba, Li, K, Fe, V, Cr, Ni, and Pb, which probably gets resuspended by the daily traffic and winds (Adamiec et al., 2016; Sanders et al., 2003).

At BON, we found two sources related to the agricultural activities, both of which are prominent in the summer. The first source is rich in As, Zn and Pb and is probably related to the application of fertilizers and herbicides. Zinc sulfate is a commonly used weed killer. Commercial

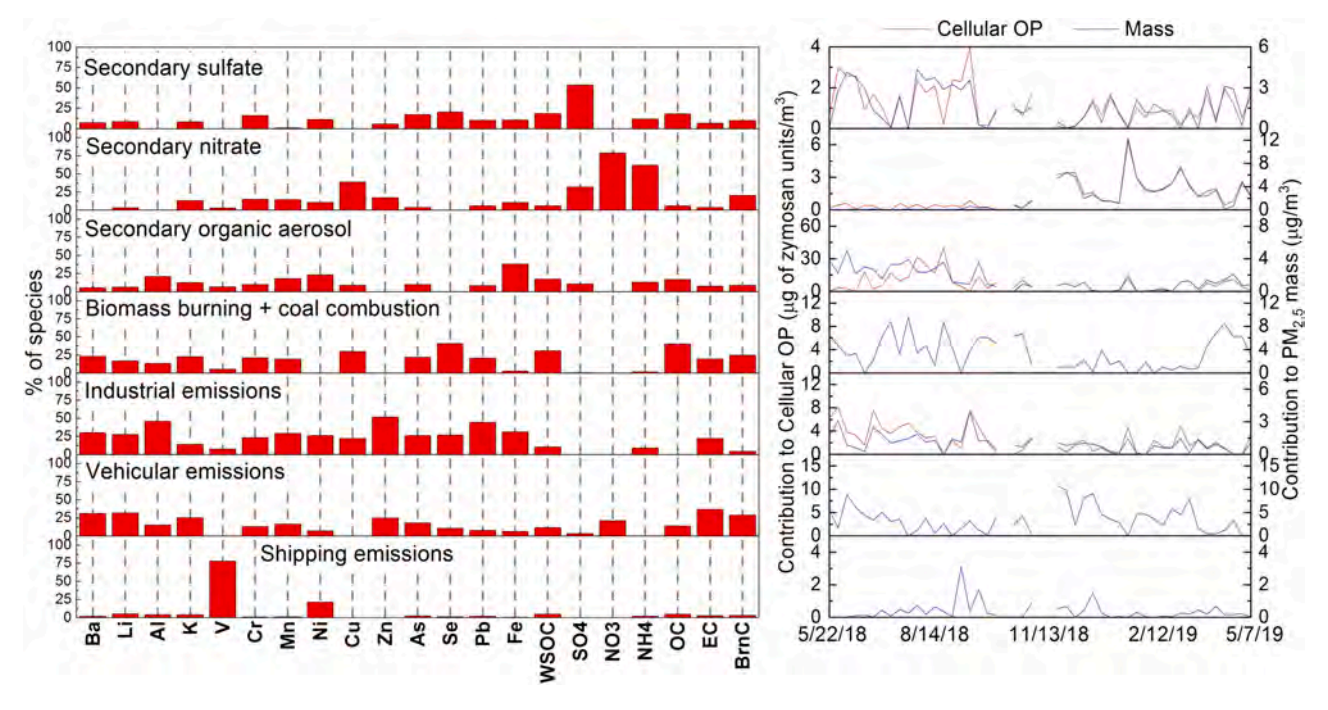


Fig. 7. Composition profiles (percentage of each species) for the various factors resolved by PMF (left panel), and the time series of their relative contribution (right panel) at STL. Composition profiles for the PMF based on both $PM_{2.5}$ mass and cellular OP were almost similar.

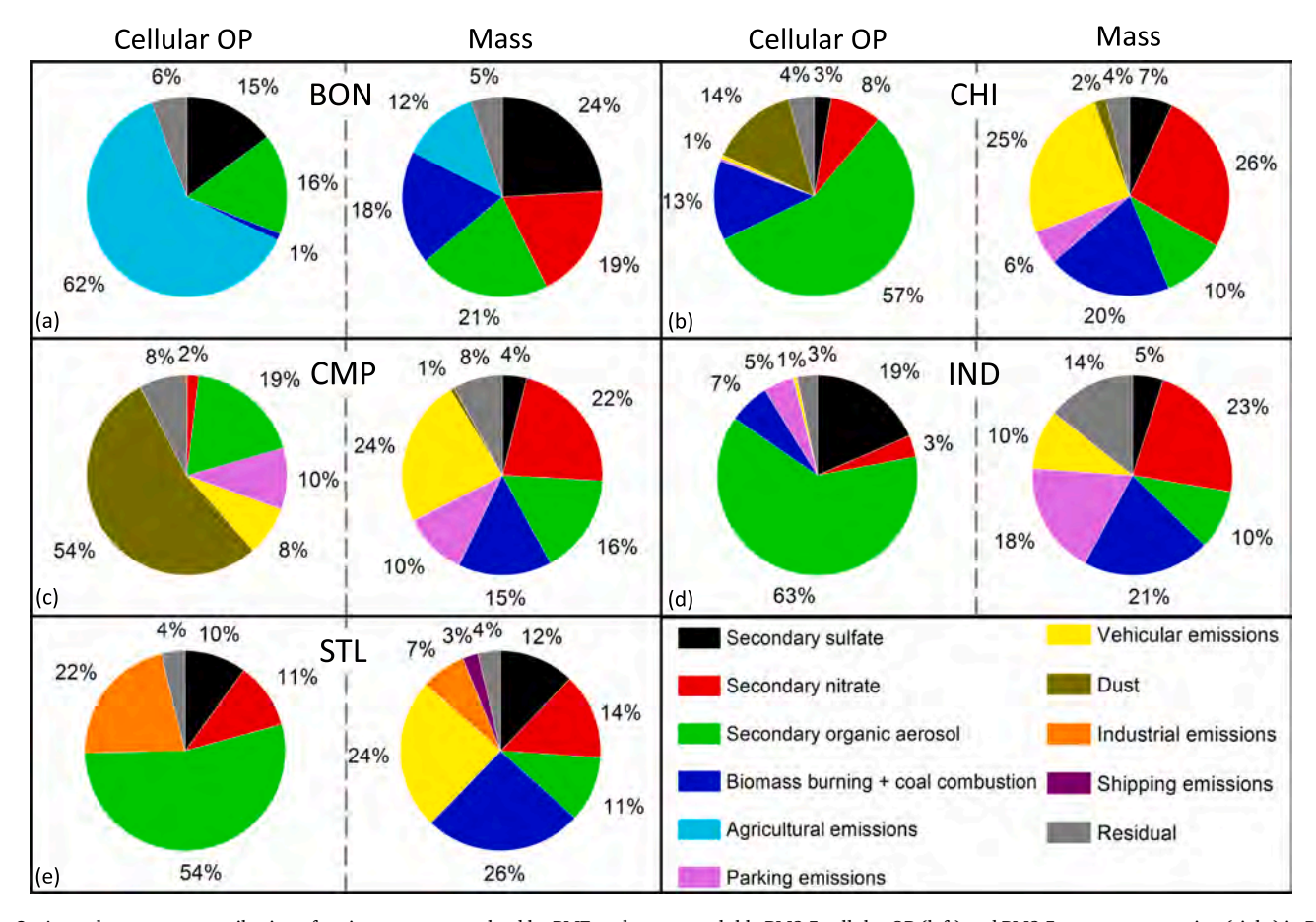


Fig. 8. Annual aggregate contribution of various sources resolved by PMF to the water-soluble PM2.5 cellular OP (left) and PM2.5 mass concentration (right) in BON (a), CHI (b), CMP (c), IND (d), and STL (e).

phosphate fertilizers contain small amounts of heavy-metal contaminants, such as As, Pb, Cr and V, which are minor constituents of the phosphate rock (Charter et al., 1995; Kruger et al., 2017; Macedo et al., 2009; Moskalyk and Alfantazi, 2003). Note, BON PM2.5's Pb concentration is the highest among five locations, which can be explained by the surrounding agricultural fields. Other important components of the fertilizers such as Se (Chen et al., 2002), NH₄⁺ (Zarebska et al., 2015), and Fe (He et al., 2013) were also abundantly present in this source. The second source is probably associated with the use of fungicides including the wear of agricultural instruments used in spraying it. Its activity lasted from June to August, having two peaks during that time. This source accounted for more than 60% of the water-soluble ambient Ni, which is probably associated with the wear of Ni-resist water pump commonly used in the sprayers. Also, copper fungicide, which is one of the most widely used fungicide (Melendez et al., 2020), is largely sprayed through the aircrafts, probably resulting into abundant Cu in this factor. Shipping emissions in STL was characterized by V (Peltier and Lippmann, 2010; Zhao et al., 2021). An industrial emission source in STL was also characterized by various abundant metals (i.e., Zn, Pb, Fe, Al, Cu, Mn and Cr). One of St. Louis's largest industrial zone, consisting of several industries such as steel manufacturing companies, salt manufacturers, metal-recycling industries, etc., is located on the east side of our sampling site, probably contributing to these elements. Together, all these emission sources explained more than 85% of both cellular OP_v and PM_{2.5} mass at all the sites $[R^2 > 0.70$, except CMP $(R^2 = 0.56$ for cellular OPv); not shown], demonstrating the robustness of our PMF

3.4.2. Source contribution to water-soluble cellular OP_{ν} vs. $PM_{2.5}$ mass concentration

Fig. 8 shows the contribution of various sources to water-soluble cellular OP_v. For comparison, the contributions of these sources to the PM_{2.5} mass are also shown in the same figure. The most important feature of this figure is a clear contrast between the contribution of various sources to the PM_{2.5} mass vs. OP. At BON, secondary sulfate, secondary nitrate, SOA, and biomass burning + coal combustion accounted for more than 80% of the PM_{2.5} mass concentration, while the agricultural sources (both fertilizers and sprayer emissions) contributed to only 12% of the PM2.5 mass. On the other hand, the combined contribution of secondary sulfate and nitrate, biomass burning + coal combustion, and SOA to the water-soluble cellular OP_v was only32%, while agricultural activities contributed 62% to the cellular OP_v. These results are somewhat consistent with two previous studies conducted at the same BON site showing a dominant contribution of secondary sources to the PM_{2.5} mass (Buzcu-Guven et al., 2007; Kim et al., 2005). However, the cellular OP_v results of our study show an important finding that despite a minor contribution to PM2.5 mass, health risks of the agricultural activities cannot be ignored.

At the roadside site (CMP), vehicular emissions is the most important contributor to $PM_{2.5}$ mass (24%), followed by secondary nitrate (22%), SOA (16%), and biomass burning + coal combustion (15%). However, among all these sources, only SOA had a significant contribution (18%), with vehicular emission contributing to only 8% to the $PM_{2.5}$ cellular $OP_{v}.$ After SOA, road dust which contributed to only 1% to the $PM_{2.5}$ mass, contributed most (54%) to the cellular $OP_{v}.$

Secondary sulfate and nitrate, and biomass burning + coal combustion had important roles in the $PM_{2.5}$ mass concentrations at urban background locations (CHI, STL and IND), and their contributions were somewhat similar at different sites (5–12% for secondary sulfate, 20–26% for biomass burning + coal combustion, and 14–26% for the secondary nitrate). However, with a few exceptions, their contributions to the cellular OP_v were generally low (3–19% for secondary sulfate, 0–13% for biomass burning + coal combustion and 3–11% for secondary nitrate). Vehicular emissions was one of the largest contributors to $PM_{2.5}$ mass concentration at CHI (25%) and STL (24%); and it had a significant contribution at IND (10%). However, the contribution of this source to

cellular OP_v was not more than 1% at any of these sites. SOA accounted for 10-11% of PM_{2.5} mass concentrations in urban background sites. Despite this low contribution, it is interesting to note that it was the most important source of cellular OPv, with the contribution ranging from 54% to 63%. These results are strikingly similar to another source apportionment study conducted in Denver, CO (Zhang et al., 2008). In that study, multiple components (i.e., WSOC, OC, EC, metals, sulfate, etc.) were employed to identify 9 sources contributing to PM_{2.5}, among which only water-soluble carbon factor, iron source, and soil dust source had substantial contribution to the cellular OP. Collectively, these results suggest the critical roles of Fe and WSOC in PM_{2.5} cellular OP. Since both WSOC and Fe are highly correlated (Tables S9-S13 in SI) and they appeared in the same factor in our study, it is difficult to decouple their effects at this stage. However, we plan to investigate it in our future studies using mechanistic techniques. Finally, although the industrial sources in CHI (suspended dust related to industry) and STL were responsible for \leq 7% of the PM_{2.5} mass concentrations, their water-soluble cellular OPv contributions in CHI and STL are 14% and 22%, respectively. Essentially, these results indicate that the contribution of various emission sources to the PM_{2.5} mass could be substantially different than their contribution to the PM2.5-related health risks.

4. Conclusion

In this study, we investigated the spatiotemporal variation and sources of water-soluble PM_{2.5} cellular OP in the mid-western US. The PM_{2.5} cellular OP in the Midwest US is spatially homogenous but showed a strong seasonal profile with the highest levels for both massnormalized and volume-normalized OP in summer and lowest levels in winter. Interestingly, cellular OP in the rural site were at a similar level as that in urban and roadside sites. It indicates that the health risks associated with ambient PM2.5 exposure in rural locations are not necessarily lesser than in the urbanized regions. The volume-normalized cellular OP generally showed a poor correlation with the PM_{2.5} mass suggesting a more dominant role of the chemical composition in driving the OP levels than the PM_{2.5} mass. This was further evident from the correlation of various chemical components with the cellular OP. Among various chemical components analyzed in our study, only few components, i.e., WSOC and Fe were consistently and strongly correlated with the cellular OP. However certain components such as Pb, Al, Cu, and Mn showed some seasonal correlations with the cellular OP particularly during winter and fall. The source apportionment conducted for both cellular OP and PM2.5 mass revealed some common sources such as secondary formation, biomass burning and coal combustion at all the sites, while some local emissions, e.g., agricultural activities, dust and industries, contributed only at the specific sites. Most importantly, the sources showed highly divergent profiles for their contribution to cellular OP vs. $PM_{2.5}$ mass at all the sites. Agricultural activities contributed to only 12% to the PM_{2.5} mass at the rural site but it was the largest contributor (62%) to cellular OP at that location. On the other hand, SOA was the largest contributor to the cellular OP at most urban sites (> 54%), despite its contribution to PM_{2.5} was not more than 11% at any of those sites. The presence of certain metals particularly Fe in the SOA source and its tight correlation with WSOC, indicates a possible role of Fe-complexes with organic compounds in driving the macrophage ROS generation, which should be explored in the future studies. Overall, our study indicates that the sources contributing substantially to PM_{2.5} mass are not necessarily equally important in terms of their health effects and source apportionment analysis should include more health-relevant metric such as OP or toxicity in their designs.

CRediT authorship contribution statement

Yixiang Wang: Conceptualization, Methodology, Validation, Formal analysis, Investigation, Resources, Writing – original draft, Visualization. **Joseph V Puthussery:** Resources, Investigation,

Reviewing. **Haoran Yu:** Resources, Investigation, Reviewing. **Yicen Liu:** Investigation. **Sudheer Salana:** Investigation, Reviewing. **Vishal Verma:** Conceptualization, Resources, Writing – review & editing, Supervision, Project administration, Funding acquisition.

Declaration of Competing Interest

The authors declare that they have no known competing financial interests or personal relationships that could have appeared to influence the work reported in this paper.

Acknowledgments

This work was supported by the National Science Foundation, USA under Grant No. CBET-1847237. We thank Sandra McMasters, the director of cell media facility at UIUC for providing us NR8383 cell culture media. We also appreciate Prof. William Harold Witola from UIUC for sharing the NR8383 cells with us.

Appendix A. Supporting information

Supplementary data associated with this article can be found in the online version at doi:10.1016/j.jhazmat.2021.127777.

References

- Adamiec, E., Jarosz-Krzeminska, E., Wieszala, R., 2016. Heavy metals from non-exhaust vehicle emissions in urban and motorway road dusts. Environ. Monit. Assess. 188 (6) https://doi.org/10.1007/s10661-016-5377-1.
- Al Hanai, A.H., Antkiewicz, D.S., Hemming, J.D.C., Shafer, M.M., Lai, A.M., Arhami, M., Hosseini, V., Schauer, J.J., 2019. Seasonal variations in the oxidative stress and inflammatory potential of PM2.5 in Tehran using an alveolar macrophage model; the role of chemical composition and sources. Environ. Int. 123, 417–427. https://doi.org/10.1016/j.envint.2018.12.023.
- Al-Masri, M.S., Al-Kharfan, K., Al-Shamali, K., 2006. Speciation of Pb, Cu and Zn determined by sequential extraction for identification of air pollution sources in Syria. Atmos. Environ. 40 (4), 753–761. https://doi.org/10.1016/j.atmosenv.2005.10.008
- Amato, F., Hopke, P.K., 2012. Source apportionment of the ambient PM2.5 across St. Louis using constrained positive matrix factorization. Atmos. Environ. 46, 329–337. https://doi.org/10.1016/j.atmosenv.2011.09.062.
- Apeagyei, E., Bank, M.S., Spengler, J.D., 2011. Distribution of heavy metals in road dust along an urban-rural gradient in Massachusetts. Atmos. Environ. 45 (13), 2310–2323. https://doi.org/10.1016/j.atmosenv.2010.11.015.
- Bates, J.T., Weber, R.J., Abrams, J., Verma, V., Fang, T., Klein, M., Strickland, M.J., Sarnat, S.E., Chang, H.H., Mulholland, J.A., Tolbert, P.E., Russell, A.G., 2015. Reactive oxygen species generation linked to sources of atmospheric particulate matter and cardiorespiratory effects. Environ. Sci. Technol. 49, 13605–13612.
- Birch, M.E., Cary, R.A., 1996. Elemental carbon-based method for monitoring occupational exposures to particulate diesel exhaust. Aerosol Sci. Tech. 25 (3), 221–241.
- Bond, T.C., Streets, D.G., Yarber, K.F., Nelson, S.M., Woo, J.H., Klimont, Z., 2004. A technology-based global inventory of black and organic carbon emissions from combustion. J. Geophys Res. Atmos. 109 (D14) https://doi.org/Artn D1420310.1029/2003jd003697.
- Brehmer, C., Norris, C., Barkjohn, K.K., Bergin, M.H., Zhang, J.F., Cui, X.X., Teng, Y.B., Zhang, Y.P., Black, M., Li, Z., Shafer, M.M., Schauer, J.J., 2020. The impact of household air cleaners on the oxidative potential of PM2.5 and the role of metals and sources associated with indoor and outdoor exposure. Environ. Res. 181 https://doi.org/ARTN108919.10.1016/j.envres.2019.108919.
- Buzcu-Guven, B., Brown, S.G., Frankel, A., Hafner, H.R., Roberts, P.T., 2007. Analysis and apportionment of organic carbon and fine particulate matter sources at multiple sites in the Midwestern United States. J. Air Waste Manag. Assoc. 57 (5), 606–619. https://doi.org/10.3155/1047-3289.57.5.606.
- Cesaroni, G., Forastiere, F., Stafoggia, M., Andersen, Z.J., Badaloni, C., Beelen, R., Caracciolo, B., de Faire, U., Erbel, R., Eriksen, K.T., Fratiglioni, L., Galassi, C., Hampel, R., Heier, M., Hennig, F., Hilding, A., Hoffmann, B., Houthuijs, D., Jockel, K.H., Korek, M., Lanki, T., Leander, K., Magnusson, P.K.E., Migliore, E., Ostenson, C.G., Overvad, K., Pedersen, N.L., Pekkanen, J.J., Penell, J., Pershagen, G., Pyko, A., Raaschou-Nielsen, O., Ranzi, A., Ricceri, F., Sacerdote, C., Salomaa, V., Swart, W., Turunen, A.W., Vineis, P., Weinmayr, G., Wolf, K., de Hoogh, K., Hoek, G., Brunekreef, B., Peters, A., 2014. Long term exposure to ambient air pollution and incidence of acute coronary events: prospective cohort study and meta-analysis in 11 European cohorts from the ESCAPE Project. BMJ Brit. Med. J. 348 https://doi.org/ARTNf7412 10.1136/bmj.f7412.
- Charrier, J.G., McFall, A.S., Richards-Henderson, N.K., Anastasio, C., 2014. Hydrogen peroxide formation in a surrogate lung fluid by transition metals and quinones

- present in particulate matter. Environ. Sci. Technol. 48 (12), 7010–7017. https://doi.org/10.1021/es501011w.
- Charrier, J.G., Richards-Henderson, N.K., Bein, K.J., McFall, A.S., Wexler, A.S., Anastasio, C., 2015. Oxidant production from source-oriented particulate matterpart 1: oxidative potential using the dithiothreitol (DTT) assay. Atmos. Chem. Phys. 15 (5), 2327–2340. https://doi.org/10.5194/acp-15-2327-2015.
- Charter, R.A., Tabatabai, M.A., Schafer, J.W., 1995. Arsenic, molybdenum, selenium, and tungsten contents of fertilizers and phosphate rocks. Commun. Soil Sci. Plan 26 (17–18), 3051–3062 https://doi.org/Doi 10.1080/00103629509369508.
- Chen, H., Kwong, J.C., Copes, R., Tu, K., Villeneuve, P.J., van Donkelaar, A., Hystad, P., Martin, R.V., Murray, B.J., Jessiman, B., Wilton, A.S., Kopp, A., Burnett, R.T., 2017. Living near major roads and the incidence of dementia, Parkinson's disease, and multiple sclerosis: a population-based cohort study. Lancet 389 (10070), 718–726. https://doi.org/10.1016/S0140-6736(16)32399-6.
- Chen, L.C., Yang, F.M., Xu, J., Hu, Y., Hu, Q.H., Zhang, Y.L., Pan, G.X., 2002. Determination of selenium concentration of rice in China and effect of fertilization of selenite and selenate on selenium content of rice. J. Agr. Food Chem. 50 (18), 5128–5130. https://doi.org/10.1021/jf0201374.
- Cheng, Y., He, K.B., Du, Z.Y., Engling, G., Liu, J.M., Ma, Y.L., Zheng, M., Weber, R.J., 2016. The characteristics of brown carbon aerosol during winter in Beijing. Atmos. Environ. 127, 355–364. https://doi.org/10.1016/j.atmosenv.2015.12.035.
- Cheung, K., Shafer, M.M., Schauer, J.J., Sioutas, C., 2012. Diurnal trends in oxidative potential of coarse particulate matter in the los angeles basin and their relation to sources and chemical composition. Environ. Sci. Technol. 46 (7), 3779–3787. https://doi.org/10.1021/es204211v.
- Chow, J.C., Watson, J.G., Lowenthal, D.H., Chen, L.W.A., Motallebi, N., 2010. Black and organic carbon emission inventories: review and application to california. J. Air Waste Manag. Assoc. 60 (4), 497–507. https://doi.org/10.3155/1047-3289 60 4 497
- Dai, Q.L., Schulze, B.C., Bi, X.H., Bui, A.A.T., Guo, F.Z., Wallace, H.W., Sanchez, N.P., Flynn, J.H., Lefer, B.L., Feng, Y.C., Griffin, R.J., 2019. Seasonal differences in formation processes of oxidized organic aerosol near Houston, TX. Atmos. Chem. Phys. 19 (14), 9641–9661. https://doi.org/10.5194/acp-19-9641-2019.
- Delfino, R.J., Staimer, N., Tjoa, T., Gillen, D.L., Schauer, J.J., Shafer, M.M., 2013. Airway inflammation and oxidative potential of air pollutant particles in a pediatric asthma panel. J. Expo. Sci. Environ. Epidemiol. 23 (5), 466–473 https://doi.org/Doi 10.1038/Jes.2013.25.
- Deng, X.B., Zhang, F., Rui, W., Long, F., Wang, L.J., Feng, Z.H., Chen, D.L., Ding, W.J., 2013. PM2.5-induced oxidative stress triggers autophagy in human lung epithelial A549 cells. Toxicol. Vitr. 27 (6), 1762–1770. https://doi.org/10.1016/j. tiv.2013.05.004.
- Duan, J., Huang, R.J., Lin, C.S., Dai, W.T., Wang, M., Gu, Y.F., Wang, Y., Zhong, H.B., Zheng, Y., Ni, H.Y., Dusek, U., Chen, Y., Li, Y.J., Chen, Q., Worsnop, D.R., O'Dowd, C.D., Cao, J.J., 2019. Distinctions in source regions and formation mechanisms of secondary aerosol in Beijing from summer to winter. Atmos. Chem. Phys. 19 (15), 10319–10334. https://doi.org/10.5194/acp-19-10319-2019.
- EPA, 2021. Air Quality National Summary ((https://www.epa.gov/air-trends/air-quality-national-summary)). https://doi.org/ (https://www.epa.gov/air-trends/air-quality-national-summary).
- Fang, T., Verma, V., Bates, J.T., Abrams, J., Klein, M., Strickland, M.J., Sarnat, S.E., Chang, H.H., Mulholland, J.A., Tolbert, P.E., Russell, A.G., Weber, R.J., 2016. Oxidative potential of ambient water-soluble PM2.5 in the southeastern United States: contrasts in sources and health associations between ascorbic acid (AA) and dithiothreitol (DTT) assays. Atmos. Chem. Phys. 16 (6), 3865–3879.
- Fann, N., Coffman, E., Timin, B., Kelly, J.T., 2018. The estimated change in the level and distribution of PM2.5-attributable health impacts in the United States: 2005-2014. Environ. Res. 167, 506–514. https://doi.org/10.1016/j.envres.2018.08.018.
- Feng, S.L., Gao, D., Liao, F., Zhou, F.R., Wang, X.M., 2016. The health effects of ambient PM2.5 and potential mechanisms. Ecotoxicol. Environ. Saf. 128, 67–74. https://doi. org/10.1016/j.ecoenv.2016.01.030.
- Galbreath, K.C., Zygarlicke, C.J., 2004. Formation and chemical speciation of arsenicchromium-, and nickel-bearing coal combustion PM2.5. Fuel Process Technol. 85 (6–7), 701–726. https://doi.org/10.1016/j.fuproc.2003.11.015.
- Garcia, C.A., Yap, P.S., Park, H.Y., Weller, B.L., 2016. Association of long-term PM2.5 exposure with mortality using different air pollution exposure models: impacts in rural and urban California. Int. J. Environ. Heal Res. 26 (2), 145–157. https://doi.org/10.1080/09603123.2015.1061113.
- Grigoratos, T., Martini, G., 2015. Brake wear particle emissions: a review. Environ. Sci. Pollut. Res. 22 (4), 2491–2504. https://doi.org/10.1007/s11356-014-3696-8.
- Hamad, S.H., Schauer, J.J., Antkiewicz, D.S., Shafer, M.M., Kadhim, A.K.H., 2016. ROS production and gene expression in alveolar macrophages exposed to PM2.5 from Baghdad, Iraq: seasonal trends and impact of chemical composition. Sci. Total Environ. 543, 739–745. https://doi.org/10.1016/j.scitotenv.2015.11.065.
- He, W.L., Shohag, M.J.I., Wei, Y.Y., Feng, Y., Yang, X.E., 2013. Iron concentration, bioavailability, and nutritional quality of polished rice affected by different forms of foliar iron fertilizer. Food Chem. 141 (4), 4122–4126. https://doi.org/10.1016/j. foodchem.2013.07.005.
- Hecobian, A., Zhang, X., Zheng, M., Frank, N., Edgerton, E.S., Weber, R.J., 2010. Water-Soluble Organic Aerosol material and the light-absorption characteristics of aqueous extracts measured over the Southeastern United States. Atmos. Chem. Phys. 10 (13), 5965–5977.
- Hiura, T.S., Kaszubowski, M.P., Li, N., Nel, A.E., 1999. Chemicals in diesel exhaust particles generate reactive oxygen radicals and induce apoptosis in macrophages. J. Immunol. 163 (10), 5582–5591.
- Holst, G.J., Pedersen, C.B., Thygesen, M., Brandt, J., Geels, C., Bonlokke, J.H., Sigsgaard, T., 2020. Air pollution and family related determinants of asthma onset

- and persistent wheezing in children: nationwide case-control study. BMJ Brit. Med. J. 370 https://doi.org/ARTNm2791.10.1136/bmj.m2791.
- Hu, S., Polidori, A., Arhami, M., Shafer, M.M., Schauer, J.J., Cho, A., Sioutas, C., 2008. Redox activity and chemical speciation of size fractioned PM in the communities of the Los Angeles-Long Beach harbor. Atmos. Chem. Phys. 8 (21), 6439–6451 https:// doi.org/DOI 10.5194/acp-8-6439-2008.
- Hu, X.F., Belle, J.H., Meng, X., Wildani, A., Waller, L.A., Strickland, M.J., Liu, Y., 2017. Estimating PM2.5 concentrations in the conterminous United States using the random forest approach. Environ. Sci. Technol. 51 (12), 6936–6944. https://doi. org/10.1021/acs.est.7b01210.
- Huang, K., Liang, F.C., Yang, X.L., Liu, F.C., Li, J.X., Xiao, Q.Y., Chen, J.C., Liu, X.Q., Cao, J., Shen, C., Yu, L., Lu, F.H., Wu, X.P., Zhao, L.C., Wu, X.G., Li, Y., Hu, D.S., Huang, J.F., Liu, Y., Lu, X.F., Gu, D.F., 2019. Long term exposure to ambient fine particulate matter and incidence of stroke: prospective cohort study from the China-PAR project. BMJ Brit. Med. J. 367 https://doi.org/ARTN 1672010.1136/bmj.16720.
- Huggins, F.E., Senior, C.L., Chu, P., Ladwig, K., Huffman, G.P., 2007. Selenium and arsenic speciation in fly ash from full-scale coal-burning utility plants. Environ. Sci. Technol. 41 (9), 3284–3289. https://doi.org/10.1021/es062069y.
- Kanda, J., 1995. Determination of ammonium in seawater based on the indophenol reaction with O-phenylphenol (Opp). Water Res. 29 (12), 2746–2750 https://doi. org/Doi 10.1016/0043-1354(95)00149-F.
- Kim, E., Hopke, P.K., Kenski, D.M., Koerber, M., 2005. Sources of fine particles in a rural midwestern U.S. area. Environ. Sci. Technol. 39 (13), 4953–4960. https://doi.org/ 10.1021/es0490774.
- Kirillova, E.N., Marinoni, A., Bonasoni, P., Vuillermoz, E., Facchini, M.C., Fuzzi, S., Decesari, S., 2016. Light absorption properties of brown carbon in the high Himalayas. J. Geophys. Res. Atmos. 121 (16), 9621–9639. https://doi.org/10.1002/ 2016id025030.
- Krall, J.R., Mulholland, J.A., Russell, A.G., Balachandran, S., Winquist, A., Tolbert, P.E., Waller, L.A., Sarnat, S.E., 2017. Associations between source-specific fine particulate matter and emergency department visits for respiratory disease in four US cities. Environ. Health Perspect. 125 (1), 97–103.
- Kruger, O., Fiedler, F., Adam, C., Vogel, C., Senz, R., 2017. Determination of chromium (VI) in primary and secondary fertilizer and their respective precursors. Chemosphere 182, 48–53. https://doi.org/10.1016/j.chemosphere.2017.05.011.
- Kumagai, Y., Koide, S., Taguchi, K., Endo, A., Nakai, Y., Yoshikawa, T., Shimojo, N., 2002. Oxidation of proximal protein sulfhydryls by phenanthraquinone, a component of diesel exhaust particles. Chem. Res. Toxicol. 15 (4), 483–489. https://doi.org/10.1021/tx0100993.
- Kundu, S., Stone, E.A., 2014. Composition and sources of fine particulate matter across urban and rural sites in the Midwestern United States. Environ. Sci. Proc. Imp. 16 (6), 1360–1370. https://doi.org/10.1039/c3em00719g.
- Lack, D.A., Langridge, J.M., Bahreini, R., Cappa, C.D., Middlebrook, A.M., Schwarz, J.P., 2012. Brown carbon and internal mixing in biomass burning particles. Proc. Natl. Acad. Sci. U.S.A. 109 (37), 14802–14807. https://doi.org/10.1073/ pnas.1206575109.
- Landreman, A.P., Shafer, M.M., Hemming, J.C., Hannigan, M.P., Schauer, J.J., 2008.
 A macrophage-based method for the assessment of the reactive oxygen species (ROS) activity of atmospheric particulate matter (PM) and application to routine (daily-24h) aerosol monitoring studies. Aerosol Sci. Technol. 42 (11), 946–957.
- Lee, J.H., Hopke, P.K., 2006. Apportioning sources of PM2.5 in St. Louis, MO using speciation trends network data. Atmos. Environ. 40, S360–S377. https://doi.org/ 10.1016/j.atmosenv.2005.11.074.
- Legan, M., 2020. Retirement of Major Indiana Coal Plant Indicates Shift Toward Sustainable Energy Future. Indiana Public Media (https://doi.org/https:// indianapublicmedia.org/news/power-plant-retirement-pushing-indiana-towardsustainable-future.php)
- Li, J., Posfai, M., Hobbs, P.V., Buseck, P.R., 2003. Individual aerosol particles from biomass burning in southern Africa: 2, Compositions and aging of inorganic particles. J. Geophys. Res. Atmos. 108 (D13) https://doi.org/Artn 8484 10.1029/ 2002id002310.
- Li, N., Sioutas, C., Cho, A., Schmitz, D., Misra, C., Sempf, J., Wang, M.Y., Oberley, T., Froines, J., Nel, A., 2003. Ultrafine particulate pollutants induce oxidative stress and mitochondrial damage. Environ. Health Perspect. 111 (4), 455–460. https://doi.org/ 10.1289/ehp.6000.
- Liu, J., Bergin, M., Guo, H., King, L., Kotra, N., Edgerton, E., Weber, R.J., 2013. Size-resolved measurements of brown carbon in water and methanol extracts and estimates of their contribution to ambient fine-particle light absorption. Atmos. Chem. Phys. 13 (24), 12389–12404. https://doi.org/10.5194/acp-13-12389-2013.
- Liu, L., Bei, N.F., Hu, B., Wu, J.R., Liu, S.X., Li, X., Wang, R.N., Liu, Z.R., Shen, Z.X., Li, G. H., 2020. Wintertime nitrate formation pathways in the north China plain: Importance of N2O5 heterogeneous hydrolysis. Environ. Pollut. 266 https://doi.org/ARTN 11528710.1016/j.envpol.2020.115287.
- Liu, Q.Y., Lu, Z.J., Xiong, Y., Huang, F., Zhou, J.B., Schauer, J.J., 2020. Oxidative potential of ambient PM2.5 in Wuhan and its comparisons with eight areas of China. Sci. Total Environ. 701 https://doi.org/ARTN134844/10.1016/j. scitotenv.2019.134844.
- Liu, W.J., Xu, Y.S., Liu, W.X., Liu, Q.Y., Yu, S.Y., Liu, Y., Wang, X., Tao, S., 2018. Oxidative potential of ambient PM2.5 in the coastal cities of the Bohai Sea, northern China: seasonal variation and source apportionment. Environ. Pollut. 236, 514–528. https://doi.org/10.1016/j.envpol.2018.01.116.
- Ma, Y.Q., Cheng, Y.B., Qiu, X.H., Cao, G., Fang, Y.H., Wang, J.X., Zhu, T., Yu, J.Z., Hu, D., 2018. Sources and oxidative potential of water-soluble humic-like substances (HULISWS) in fine particulate matter (PM2.5) in Beijing. Atmos. Chem. Phys. 18 (8), 5607–5617. https://doi.org/10.5194/acp-18-5607-2018.

- Macedo, S.M., de Jesus, R.M., Garcia, K.S., Hatje, V., Queiroz, A.F.D., Ferreira, S.L.C., 2009. Determination of total arsenic and arsenic (III) in phosphate fertilizers and phosphate rocks by HG-AAS after multivariate optimization based on Box-Behnken design. Talanta 80 (2), 974–979. https://doi.org/10.1016/j.talanta.2009.08.025.
- Melendez, M.V., Heckman, J.R., Murphy, S., D'Amico, F., 2020. New Jersey farm soil copper levels resulting from copper fungicide applications. Horttechnology 30 (2), 268–272. https://doi.org/10.21273/Horttech04494-19.
- Milando, C., Huang, L., Batterman, S., 2016. Trends in PM2.5 emissions, concentrations and apportionments in Detroit and Chicago. Atmos. Environ. 129, 197–209. https:// doi.org/10.1016/j.atmosenv.2016.01.012.
- Miller, F.J., Gardner, D.E., Graham, J.A., Lee, R.E., Wilson, W.E., Bachmann, J.D., 1979.Size considerations for establishing a standard for inhalable particles. J. Air Pollut.Control Assoc. 29 (6), 610–615.
- Moskalyk, R.R., Alfantazi, A.M., 2003. Processing of vanadium: a review. Min. Eng. 16 (9), 793–805. https://doi.org/10.1016/S0892-6875(03)00213-9.
- Mudway, I.S., Duggan, S.T., Venkataraman, C., Habib, G., Kelly, F.J., Grigg, J., 2005.
 Combustion of dried animal dung as biofuel results in the generation of highly redox active fine particulates. Part. Fibre Toxicol. 2 (1), 6.
- Mudway, I.S., Stenfors, N., Duggan, S.T., Roxborough, H., Zielinski, H., Marklund, S.L., Blomberg, A., Frew, A.J., Sandstrom, T., Kelly, F.J., 2004. An in vitro and in vivo investigation of the effects of diesel exhaust on human airway lining fluid antioxidants. Arch. Biochem. Biophys. 423 (1), 200–212 https://doi.org/DOI 10.1016/j.abb.2003.12.018.
- Paatero, P., Tapper, U., 1993. Analysis of different modes of factor-analysis as least-squares fit problems. Chemom. Intell. Lab 18 (2), 183–194 https://doi.org/Doi 10.1016/0169-7439(93)80055-M.
- Paris, R., Desboeufs, K.V., 2013. Effect of atmospheric organic complexation on iron-bearing dust solubility. Atmos. Chem. Phys. 13 (9), 4895–4905 https://doi.org/10.5194/acp-13-4895-2013.
- Park, J., Park, E.H., Schauer, J.J., Yi, S.M., Heo, J., 2018. Reactive oxygen species (ROS) activity of ambient fine particles (PM2.5) measured in Seoul, Korea. Environ. Int. 117, 276–283 https://doi.org/10.1016/j.envint.2018.05.018.
- Peltier, R.E., Lippmann, M., 2010. Residual oil combustion: 2. Distributions of airborne nickel and vanadium within New York City. J. Expo. Sci. Environ. Epidemol. 20 (4), 342–350 https://doi.org/10.1038/jes.2009.28.
- Pun, V.C., Kazemiparkouhi, F., Manjourides, J., Suh, H.H., 2017. Long-term PM2.5 exposure and respiratory, cancer, and cardiovascular mortality in older us adults. Am. J. Epidemiol. 186 (8), 961–969 https://doi.org/10.1093/aie/kwx166.
- Raaschou-Nielsen, O., Pedersen, M., Stafoggia, M., Weinmayr, G., Andersen, Z.J., Galassi, C., Sommar, J., Forsberg, B., Olsson, D., Oftedal, B., Krog, N.H., Aasvang, G. M., Pyko, A., Pershagen, G., Korek, M., De Faire, U., Pedersen, N.L., Ostenson, C.G., Fratiglioni, L., Sorensen, M., Eriksen, K.T., Tjonneland, A., Peeters, P.H., Bueno-de-Mesquita, H.B., Plusquin, M., Key, T.J., Jaensch, A., Nagel, G., Foger, B., Wang, M., Tsai, M.Y., Grioni, S., Marcon, A., Krogh, V., Ricceri, F., Sacerdote, C., Migliore, E., Tamayo, I., Amiano, P., Dorronsoro, M., Sokhi, R., Kooter, I., de Hoogh, K., Beelen, R., Eeftens, M., Vermeulen, R., Vineis, P., Brunekreef, B., Hoek, G., 2017. Outdoor air pollution and risk for kidney parenchyma cancer in 14 European cohorts. Int. J. Cancer 140 (7), 1528–1537 https://doi.org/10.1002/ijc.30587.
- Reff, A., Bhave, P.V., Simon, H., Pace, T.G., Pouliot, G.A., Mobley, J.D., Houyoux, M., 2009. Emissions inventory of PM2.5 trace elements across the United States. Environ. Sci. Technol. 43 (15), 5790–5796 https://doi.org/10.1021/es802930x.
- Rodhe, Y., Skoglund, S., Wallinder, I.O., Potacova, Z., Moller, L., 2015. Copper-based nanoparticles induce high toxicity in leukemic HL60 cells. Toxicol. Vitr. 29 (7), 1711–1719. https://doi.org/10.1016/j.tiv.2015.05.020.
- Salana, S., Wang, Y., Puthussery, J., Verma, V., 2021. A Semi-automated Instrument for Cellular Oxidative Potential Evaluation (SCOPE) of water-soluble extracts of ambient particulate matter. Atmos. Meas. Tech. Discuss. 1–26.
- Sanders, P.G., Xu, N., Dalka, T.M., Maricq, M.M., 2003. Airborne brake wear debris: size distributions, composition, and a comparison of dynamometer and vehicle tests. Environ. Sci. Technol. 37 (18), 4060–4069 https://doi.org/10.1021/es034145s.
- Sarnat, S.E., Winquist, A., Schauer, J.J., Turner, J.R., Sarnat, J.A., 2015. Fine particulate matter components and emergency department visits for cardiovascular and respiratory diseases in the St. Louis, Missouri-Illinois, Metropolitan Area. Environ. Health Perspect. 123 (5), 437–444 https://doi.org/10.1289/ehp.1307776.
- Sauve, S., McBride, M., Hendershot, W., 1998. Soil solution speciation of lead(II): Effects of organic matter and pH. Soil Sci. Soc. Am. J. 62 (3), 618–621 https://doi.org/DOI10.2136/sssaj1998.03615995006200030010x.
- Shafer, M.M., Perkins, D.A., Antkiewicz, D.S., Stone, E.A., Quraishi, T.A., Schauer, J.J., 2010. Reactive oxygen species activity and chemical speciation of size-fractionated atmospheric particulate matter from Lahore, Pakistan: an important role for transition metals. J. Environ. Monit. 12 (3), 704–715. https://doi.org/10.1039/ b915008k.
- Shah, A.S.V., Lee, K.K., McAllister, D.A., Hunter, A., Nair, H., Whiteley, W., Langrish, J. P., Newby, D.E., Mills, N.L., 2015. Short term exposure to air pollution and stroke: systematic review and meta-analysis. BMJ Brit. Med. J. 350 https://doi.org/ARTN h129510.1136/bmj.h1295.
- Silva, P.J., Carlin, R.A., Prather, K.A., 2000. Single particle analysis of suspended soil dust from Southern California. Atmos. Environ. 34 (11), 1811–1820 https://doi.org/ Doi 10.1016/S1352-2310(99)00338-6.
- Stoiber, T.L., Shafer, M.M., Armstrong, D.E., 2013. Induction of reactive oxygen species in Chlamydomonas reinhardtii in response to contrasting trace metal exposures. Environ. Toxicol. 28 (9), 516–523. https://doi.org/10.1002/tox.20743.
- Sun, X., Wang, H.Q., Guo, Z.G., Lu, P.L., Song, F.Z., Liu, L., Liu, J.X., Rose, N.L., Wang, F. W., 2020. Positive matrix factorization on source apportionment for typical pollutants in different environmental media: a review. Environ. Sci. -Proc. Imp. 22 (2), 239–255. https://doi.org/10.1039/c9em00529c.

- Taghvaee, S., Sowlat, M.H., Diapouli, E., Manousakas, M.I., Vasilatou, V., Eleftheriadis, K., Sioutas, C., 2019. Source apportionment of the oxidative potential of fine ambient particulate matter (PM2.5) in Athens, Greece. Sci. Total Environ. 653, 1407–1416 https://doi.org/10.1016/j.scitotenv.2018.11.016.
- Tapparo, A., Di Marco, V., Badocco, D., D'Aronco, S., Solda, L., Pastore, P., Mahon, B.M., Kalberer, M., Giorio, C., 2020. Formation of metal-organic ligand complexes affects solubility of metals in airborne particles at an urban site in the Po valley. Chemosphere 241 https://doi.org/ARTN125.025.10.1016/j. chemosphere.2019.125025.
- Tian, Y.H., Liu, H., Wu, Y.Q., Si, Y.Q., Song, J., Cao, Y.Y., Li, M., Wu, Y., Wang, X.W., Chen, L.B., Wei, C., Gao, P., Hu, Y.H., 2019. Association between ambient fine particulate pollution and hospital admissions for cause specific cardiovascular disease: time series study in 184 major Chinese cities. BMJ Brit. Med. J. 367 https://doi.org/ARTN 1657210.1136/bmj.16572.
- Turner, M.C., Krewski, D., Diver, W.R., Pope, C.A., Burnett, R.T., Jerrett, M., Marshall, J. D., Gapstur, S.M., 2017. Ambient air pollution and cancer mortality in the cancer prevention study II. Environ. Health Perspect. 125 (8) https://doi.org/Unsp 087013 10.1289/Ehp1249.
- Underwood, E., 2017. The polluted brain The microscopic particles sifting from freeways and power plants don't just harm your heart and lungs. They may also attack your brain. Science 355 (6323), 342–345 https://doi.org/DOI 10.1126/ science.355.6323.342.
- Verma, V., Fang, T., Guo, H., King, L., Bates, J.T., Peltier, R.E., Edgerton, E., Russell, A. G., Weber, R.J., 2014. Reactive oxygen species associated with water-soluble PM2.5 in the southeastern United States: spatiotemporal trends and source apportionment. Atmos. Chem. Phys. 14 (23), 12915–12930 https://doi.org/10.5194/acp-14-12915-2014.
- Verma, V., Ning, Z., Cho, A.K., Schauer, J.J., Shafer, M.M., Sioutas, C., 2009a. Redox activity of urban quasi-ultrafine particles from primary and secondary sources. Atmos. Environ. 43 (40), 6360–6368.
- Verma, V., Polidori, A., Schauer, J.J., Shafer, M.M., Cassee, F.R., Sioutas, C., 2009b. Physicochemical and toxicological profiles of particulate matter in Los Angeles during the October 2007 Southern California Wildfires. Environ. Sci. Technol. 43 (3), 954–960 https://doi.org/10.1021/es8021667.
- Vidrio, E., Phuah, C.H., Dillner, A.M., Anastasio, C., 2009. Generation of hydroxyl radicals from ambient fine particles in a surrogate lung fluid solution. Environ. Sci. Technol. 43 (3), 922–927 https://doi.org/10.1021/es801653u.
- Wang, D.B., Pakbin, P., Shafer, M.M., Antkiewicz, D., Schauer, J.J., Sioutas, C., 2013. Macrophage reactive oxygen species activity of water-soluble and water-insoluble fractions of ambient coarse, PM2.5 and ultrafine particulate matter (PM) in Los Angeles. Atmos. Environ. 77, 301–310. https://doi.org/10.1016/j. atmosenv.2013.05.031.
- Wang, D.F., Zhou, B., Fu, Q.Y., Zhao, Q.B., Zhang, Q., Chen, J.M., Yang, X., Duan, Y.S., Li, J., 2016. Intense secondary aerosol formation due to strong atmospheric photochemical reactions in summer: observations at a rural site in eastern Yangtze River Delta of China. Sci. Total Environ. 571, 1454–1466. https://doi.org/10.1016/ i.scitotenv.2016.06.212.
- Wang, H.C., Lu, K.D., Chen, X.R., Zhu, Q.D., Wu, Z.J., Wu, Y.S., Sun, K., 2018. Fast particulate nitrate formation via N2O5 uptake aloft in winter in Beijing. Atmos. Chem. Phys. 18 (14), 10483–10495 https://doi.org/10.5194/acp-18-10483-2018.
- Wang, Y., Plewa, M.J., Mukherjee, U.K., Verma, V., 2018. Assessing the cytotoxicity of ambient particulate matter (PM) using Chinese hamster ovary (CHO) cells and its relationship with the PM chemical composition and oxidative potential. Atmos. Environ. 179, 132–141.
- Wang, Y.Q., Wang, M.M., Li, S.P., Sun, H.Y., Mu, Z., Zhang, L.X., Li, Y.G., Chen, Q.C., 2020. Study on the oxidation potential of the water-soluble components of ambient PM2.5 over Xi'an, China: pollution levels, source apportionment and transport pathways. Environ. Int.

- Wang, Z.H., Chen, X., Ji, H.W., Ma, W.H., Chen, C.C., Zhao, J.C., 2010. Photochemical cycling of iron mediated by dicarboxylates: special effect of malonate. Environ. Sci. Technol. 44 (1), 263–268. https://doi.org/10.1021/es901956x.
- Wei, J.L., Yu, H.R., Wang, Y.X., Verma, V., 2019. Complexation of iron and copper in ambient particulate matter and its effect on the oxidative potential measured in a surrogate lung fluid. Environ. Sci. Technol. 53 (3), 1661–1671. https://doi.org/ 10.1021/acs.est.8b05731.
- Weng, L.P., Temminghoff, E.J.M., Lofts, S., Tipping, E., Van Riemsdijk, W.H., 2002. Complexation with dissolved organic matter and solubility control of heavy metals in a sandy soil. Environ. Sci. Technol. 36 (22), 4804–4810. https://doi.org/10.1021/est/200084
- Wu, G.M., Ram, K., Fu, P.Q., Wang, W., Zhang, Y.L., Liu, X.Y., Stone, E.A., Pradhan, B.B., Dangol, P.M., Panday, A.K., Wan, X., Bai, Z.P., Kang, S.C., Zhang, Q.G., Cong, Z.Y., 2019. Water-soluble brown carbon in atmospheric aerosols from Godavari (Nepal), a regional representative of South Asia. Environ. Sci. Technol. 53 (7), 3471–3479. https://doi.org/10.1021/acs.est.9b00596.
- Yan, B., Zheng, M., Hu, Y.T., Lee, S., Kim, H.K., Russell, A.G., 2008. Organic composition of carbonaceous aerosols in an aged prescribed fire plume. Atmos. Chem. Phys. 8 (21), 6381–6394 https://doi.org/DOI 10.5194/acp-8-6381-2008.
- Ying, Q., 2011. Physical and chemical processes of wintertime secondary nitrate aerosol formation. Front. Environ. Sci. Environ. 5 (3), 348–361. https://doi.org/10.1007/ s11783-011-0343-1.
- Yu, H., Puthussery, J.V., Wang, Y., Verma, V., 2021. Spatiotemporal variability in the oxidative potential of ambient fine particulate matter in Midwestern United States. Atmos. Chem. Phys. Discuss. 1–33.
- Yu, S.Y., Liu, W.J., Xu, Y.S., Yi, K., Zhou, M., Tao, S., Liu, W.X., 2019. Characteristics and oxidative potential of atmospheric PM2.5 in Beijing: Source apportionment and seasonal variation. Sci. Total Environ. 650, 277–287. https://doi.org/10.1016/j.scitotenv.2018.09.021.
- Yudovich, Y.E., Ketris, M.P., 2005. Arsenic in coal: a review. Int. J. Coal Geol. 61 (3–4), 141–196. https://doi.org/10.1016/j.coal.2004.09.003.
- Zarebska, A., Nieto, D.R., Christensen, K.V., Sotoft, L.F., Norddahl, B., 2015. Ammonium fertilizers production from manure: a critical review. Crit. Rev. Environ. Sci. Tec. 45 (14), 1469–1521. https://doi.org/10.1080/10643389.2014.955630.
- Zhang, X., Liu, Z., Hecobian, A., Zheng, M., Frank, N.H., Edgerton, S., Weber, R.J., 2012. Spatial and seasonal variations of fine particle water-soluble organic carbon (WSOC) over the southeastern United States: implications for secondary organic aerosol formation. Atmos. Chem. Phys. 12 (14), 6593–6607. https://doi.org/10.5194/acp-12.6593-2012.
- Zhang, Y.X., Schauer, J.J., Shafer, M.M., Hannigan, M.P., Dutton, S.J., 2008. Source apportionment of in vitro reactive oxygen species bioassay activity from atmospheric particulate matter. Environ. Sci. Technol. 42 (19), 7502–7509. https://doi.org/10.1021/es800126v.
- Zhang, Y.Y., Obrist, D., Zielinska, B., Gertler, A., 2013. Particulate emissions from different types of biomass burning. Atmos. Environ. 72, 27–35. https://doi.org/ 10.1016/j.atmosenv.2013.02.026.
- Zhao, J.R., Zhang, Y., Xu, H.R., Tao, S., Wang, R., Yu, Q., Chen, Y., Zou, Z., Ma, W.C., 2021. Trace elements from ocean-going vessels in east asia: vanadium and nickel emissions and their impacts on air quality. J. Geophys Res. Atmos. 126 (8) https://doi.org/ARTNe2020.ID033984 10.1029/2020.ID033984.
- Zhu, C.S., Cao, J.J., Huang, R.J., Shen, Z.X., Wang, Q.Y., Zhang, N.N., 2018. Light absorption properties of brown carbon over the southeastern Tibetan Plateau. Sci. Total Environ. 625, 246–251. https://doi.org/10.1016/j.scitotenv.2017.12.183.
- Zielinski, H., Mudway, I.S., Berube, K.A., Murphy, S., Richards, R., Kelly, F.J., 1999.
 Modeling the interactions of particulates with epithelial lining fluid antioxidants.
 Am. J. Physiol. Lung C 277 (4), L719–L726.
- Zielinski, R.A., Foster, A.L., Meeker, G.P., Brownfield, I.K., 2007. Mode of occurrence of arsenic in feed coal and its derivative fly ash, Black Warrior Basin, Alabama. Fuel 86 (4), 560–572. https://doi.org/10.1016/j.fuel.2006.07.033.